Journal of Energy Storage 154 (2026) 121206

Contents lists available at ScienceDirect

Journal of Energy Storage

journal homepage: www.elsevier.com/locate/est

Research papers

A decentralized bi-level framework for activating flexibility services from energy storage systems, electric vehicle batteries, and integrated demand response in multi-energy networks

Leila Bagherzadeh [a], Innocent Kamwa [a], Atieh Delavari [b], Seyed Amir Mansouri [c,*]

[a] Department of Electrical Engineering, Laval University, Quebec, QC, G1V 0A6, Canada
[b] Power System Management and Control Department, Hydro-Quebec Institute of Research, Varennes, Canada
[c] Department of Engineering Systems & Services, Faculty of Technology, Policy & Management, Delft University of Technology, Delft, the Netherlands

ARTICLE INFO

Keywords:
Power-gas networks, energy hubs
Flexibility market
Integrated demand response programs
Vehicle-to-grid technologies
Distributed optimization

ABSTRACT

Energy hubs are emerging as key enablers of flexibility in modern multi-energy systems, particularly as the integration of energy storage technologies expands across residential, commercial, and industrial sectors. Their ability to coordinate distributed resources, including storage, demand response, and vehicle-to-grid (V2G) assets, offers a scalable pathway to support system reliability and local balancing needs. Realizing this potential, however, requires decentralized coordination schemes that allow hubs and system operators to collaborate without extensive data exchange, a growing necessity in competitive and privacy-sensitive environments. This study develops a decentralized bi-level optimization framework that explicitly links the operational decisions of energy hubs with the real-time management of coupled electricity and gas networks. At the upper level, the system operator supervises both infrastructures, addresses energy imbalances, and specifies the flexibility requirements to be procured from upstream networks and downstream hubs. Intra-day uncertainties in demand and renewable generation are modeled using white noise with Gaussian, Beta, and Weibull probability distributions to capture realistic operational fluctuations. At the lower level, diverse hubs autonomously schedule their storage units, controllable loads, and V2G resources to maximize the flexible services they can offer. To enhance coordination performance, an adaptive Alternating Direction Method of Multipliers (ADMM) is introduced, which reduces communication exchanges and achieves a 63.27% faster convergence compared to the classical formulation. The proposed framework is implemented in GAMS and solved with GUROBI, using a test system that couples a 118-bus electrical distribution network with a 65-node gas distribution network. Results demonstrate that the model effectively activates multi-energy flexibility from integrated demand response, energy storage systems, and electric vehicles. This coordinated flexibility increases economic benefits for hubs, reduces the system operator's operational costs by up to 19.33%, and lowers total system losses by 6.12%.

Nomenclature

Sets	
h	Energy hub index
t	Time period index
i, j	Bus/Node indices
l	Line index
es	Electrical storage system index
gs	Gas storage system index
g	Dispatchable generation unit index
s	PV unit index
w	Wind unit index
ev	Electric vehicle index
Scalars	
G_l/B_l	Line conductance/susceptance (S)
R_l	Line resistance (Ω)
S_l^F	Line thermal capacity (kVA)
S^B	Base apparent power (kVA)
$P_g^{GU,Min}/P_g^{GU,Max}$	Min/Max power of dispatchable unit g (kW)
$Q_g^{GU,Min}/Q_g^{GU,Max}$	Min/Max reactive power of unit g (kVar)
v_i^{Min}/v_i^{Max}	Min/Max voltage magnitude (p.u.)

(continued on next column)
(continued)
(continued on next page)

* Corresponding author.
E-mail address: s.mansouri@tudelft.nl (S.A. Mansouri).

https://doi.org/10.1016/j.est.2026.121206
Received 25 November 2025; Received in revised form 26 January 2026; Accepted 17 February 2026
Available online 20 February 2026

(*continued*)

$\theta_i^{Min}/\theta_i^{Max}$	Min/Max voltage angle (rad)
Pr_i^{Min}/Pr_i^{Max}	Min/Max gas pressure (bar)
$E_{es}^{ES,Min}/E_{es}^{ES,Max}$	Min/Max electrical storage capacity (kWh)
$P_{es}^{Ch,Max}/P_{es}^{Dis,Max}$	Max charging/discharging power (kW)
$V_{g_s}^{min}/V_{g_s}^{max}$	Min/Max gas storage volume (m^3)
$G_{g_s}^{max.in}/G_{g_s}^{max.out}$	Max injection/extraction rate (m^3/h)
η_{g_s}	Gas storage efficiency
$E_{ev}^{EV,Min}/E_{ev}^{EV,Max}$	Min/Max EV battery capacity (kWh)
$P_{ev}^{Ch,Max}/P_{ev}^{Dis,Max}$	Max EV charging/discharging power (kW)
η_h^{gp}/η_h^{gh}	CHP electrical/thermal efficiency
η_h^{eh}/η_h^{ec}	EHP heating/cooling coefficient of performance
η_h^{hc}	Absorption chiller coefficient of performance
η_h^{eh}	Electric heater efficiency
$\eta_{es}^{Ch}/\eta_{es}^{Dis}$	Electrical storage charging/discharging efficiency
η_h^{Boiler}	Boiler efficiency
η_s^{PV}	PV panel efficiency
LHV^G	Lower heating value of gas (kWh/m^3)
M^G	Gas molar mass (kg/kmol)
ϕ	Unit conversion factor (3.6)
$S_{ci}/S_r/S_{co}$	Cut-in/ rated/ cut-out wind speeds (m/s)
SI^R	Reference solar irradiance (W/m^2)
$P_w^{WT,Max}/P_s^{PV,Max}$	Maximum wind turbine/PV capacity (kW)
ρ_h^P/ρ_h^G	ADMM penalty coefficients for hub h
PR^P/PR^G	Primal residuals
DR^P/DR^G	Dual residuals
M	Large positive constant
Parameters	
$\tau_{i,l}^F$	Line-bus incidence parameter
$\lambda_{h,t}^{P,Hub}$	Power flexibility price from hub h ($/kW)
$\lambda_{h,t}^{G,Hub}$	Gas flexibility price from hub h ($/$m^3$)
$\pi_t^{P,EN}$	External network power flexibility price ($/kW)
$\pi_t^{G,EN}$	External network gas flexibility price ($/$m^3$)
π_g^{GU}	Dispatchable unit flexibility price ($/kW)
$\pi_{es}^{ES}/\pi_{gs}^{GS}$	Storage flexibility prices ($/kW, $/$m^3$)
S_t	Wind speed at time t (m/s)
SI_t	Solar irradiance at time t (W/m^2)
$\delta_{i,t}^D/\delta_{s,t}^{PV}/\delta_{w,t}^{WT}$	Noise factors for load demand, PV generation, and wind generation
$P_h^A/P_h^B/P_h^C/P_h^D$	Power coordinates of CHP feasible region vertices A, B, C, D in hub h (kW)
$H_h^A/H_h^B/H_h^C/H_h^D$	Heat coordinates of CHP feasible region vertices A, B, C, D in hub h (kW)
Variables	
$P_{l,t}^F/Q_{l,t}^F$	Active/Reactive power flow in line l at time t (kW/kVar)
$P_{l,t}^L$	Active power losses in line l at time t (kW)
$v_{i,t}/\theta_{i,t}$	Voltage magnitude/angle at bus i at time t (p.u./rad)
$\overline{P}_{g,t}^{GU}/Q_{g,t}^{GU}$	Day-ahead active/ reactive power output schedule of unit g (kW/kVar)
$P_{g,t}^{GU,U}/P_{g,t}^{GU,D}$	Upward/downward power flexibility from unit g (kW)
$P_t^{EN,U}/P_t^{EN,D}$	Upward/downward power from external network (kW)
$P_{es,t}^{ES,U}/P_{es,t}^{ES,D}$	Upward/downward power from electrical storage (kW)
$P_{s,t}^{PV}$	PV power output of unit s at time t (kW)
$P_{w,t}^{WT}$	Wind power output of unit w at time t (kW)
$\overline{P}_{s,t}^{Solar}$	Day-ahead PV power schedule (kW)
$\overline{P}_{w,t}^{Wind}$	Day-ahead wind power schedule (kW)
$G_{l,t}^F$	Gas flow in pipeline l at time t (m^3/h)
$Pr_{i,t}$	Gas pressure at node i at time t (bar)
$\overline{G}_{g,t}^{GU}$	Day-ahead gas consumption schedule of unit g (m^3/h)
$G_{g,t}^{GU,U}/G_{g,t}^{GU,D}$	Upward/downward gas flexibility from unit g (m^3/h)
$G_t^{EN,U}/G_t^{EN,D}$	Upward/downward gas from external network (m^3/h)
$G_{gs,t}^{GS,U}/G_{gs,t}^{GS,D}$	Upward/downward gas from gas storage (m^3/h)
$\overline{G}_{i,t}^D$	Day-ahead gas demand at node i (m^3/h)
$\widetilde{P}_{h,t}^{Hub}$	Hub h power exchange (optimization variable) (kW)
$\widetilde{G}_{h,t}^{Hub}$	Hub h gas consumption (optimization variable) (m^3/h)
$\overline{P}_{h,t}^{Hub}$	Day-ahead power exchange schedule of hub h (kW)
$\overline{G}_{h,t}^{Hub}$	Day-ahead gas consumption schedule of hub h (m^3/h)
$P_{h,t}^{Hub,U}/P_{h,t}^{Hub,D}$	Hub h upward/downward power flexibility (kW)

(*continued on next column*)

(*continued*)

$G_{h,t}^{Hub,U}/G_{h,t}^{Hub,D}$	Hub h upward/downward gas flexibility (m^3/h)
$P_{h,t}^{CHP}/H_{h,t}^{CHP}$	CHP electrical/thermal output in hub h (kW)
$G_{h,t}^{CHP}$	CHP gas consumption in hub h (m^3/h)
$H_{h,t}^{Boiler}$	Boiler thermal output in hub h (kW)
$G_{h,t}^{Boiler}$	Boiler gas consumption in hub h (m^3/h)
$P_{h,t}^{EHP}$	EHP power consumption in hub h (kW)
$H_{h,t}^{EHP}/C_{h,t}^{EHP}$	EHP heating/cooling output in hub h (kW)
$C_{h,t}^{AC}$	Absorption chiller cooling output in hub h (kW)
$H_{h,t}^{AC}$	Heat input to absorption chiller in hub h (kW)
$P_{h,t}^{EH}$	Electric heater power consumption in hub h (kW)
$H_{h,t}^{EH}$	Electric heater thermal output in hub h (kW)
$E_{es,t}^{ES}$	Electrical storage energy level at time t (kWh)
$P_{es,t}^{Ch}/P_{es,t}^{Dis}$	Electrical storage charging/discharging power (kW)
$P_{es,t}^{ES}$	Net electrical storage power exchange (kW)
$V_{g_s,t}$	Gas storage volume at time t (m^3)
$G_{g_s,t}^{in}/G_{g_s,t}^{out}$	Gas injection/extraction rate at time t (m^3/h)
$E_{ev,t}^{EV}$	EV battery energy level at time t (kWh)
$P_{ev,t}^{Ch}/P_{ev,t}^{Dis}$	EV charging/discharging power (kW)
$E_{es,t=0}^{ES}/E_{es,t=T}^{ES}$	Initial and final electrical storage energy (kWh)
$E_{ev}^{EV,Ar}/E_{ev}^{EV,Dp}$	EV arrival and departure energy levels (kWh)
$L_{h,t}^P/L_{h,t}^H/L_{h,t}^C$	Electrical/heating/cooling load of hub h at time t (kW)
$L_{h,t}^{P,+}/L_{h,t}^{P,-}$	Electrical load shift-up/down (kW)
$L_{h,t}^{H,+}/L_{h,t}^{H,-}$	Heating load shift-up/down (kW)
$L_{h,t}^{C,+}/L_{h,t}^{C,-}$	Cooling load shift-up/down (kW)
$\lambda_{h,t}^{P,Hub}/\lambda_{h,t}^{G,Hub}$	ADMM dual variables
Binary Variables	
$I_{g,t}^{GU}$	On/Off status of dispatchable unit g at time t
$I_{es,t}^{Ch}$	Charging status of electrical storage es at time t
$I_{ev,t}^{Ch}$	EV charging status at time t
$I_{h,t}^{CHP}$	CHP operational mode in hub h at time t
$I_{h,t}^{EHP}$	EHP operational mode in hub h *at time* t
$I_{h,t}^{P/H/C,+}/I_{h,t}^{P/H/C,-}$	Load shift-up/down for power/heating/cooling in hub h
$I_t^{P,U}/I_t^{P,D}$	Upward/downward power flexibility requirement indicators
$I_t^{G,U}/I_t^{G,D}$	Upward/downward gas flexibility requirement indicators

1. Introduction

1.1. Background and motivations

The increasing integration of renewable energy sources and the growing complexity of energy systems have heightened the need for advanced flexibility solutions to ensure system reliability and cost-effective operation [1,2]. Energy hubs, as multi-energy management entities, play a crucial role in providing such flexibility by coordinating various Distributed Energy Resources (DERs), including controllable loads, energy storage systems, and V2G technologies [3,4]. These hubs can dynamically adjust their energy consumption, storage, and injection patterns to respond to grid conditions, offering essential flexibility to coupled power and gas networks [5]. In this context, flexibility markets have emerged as a key mechanism for monetizing and optimizing the participation of energy hubs in system balancing and congestion management [6,7]. By leveraging IDR, storage, and V2G, energy hubs can provide fast-response services to mitigate fluctuations in renewable generation and enhance grid resilience. However, effectively coordinating the participation of energy hubs in flexibility markets presents significant challenges due to their decentralized nature, complex interdependencies, and the operational constraints of coupled power and gas networks [8]. To address these challenges, distributed optimization techniques have gained traction as a promising approach for achieving secure and efficient coordination between energy hubs and the system operator [9]. Unlike centralized methods, which require full system information and result in high computational burdens, distributed optimization enables local decision-making while ensuring global feasibility and optimality through coordinated interactions [10]. Such

techniques preserve data privacy, reduce computational complexity, and allow energy hubs to autonomously manage their flexibility while contributing to overall system stability [11,12].

Motivated by the critical role of energy hubs in flexibility markets and the challenges of secure coordination, the authors of this paper propose a novel distributed optimization framework for the participation of energy hubs in flexibility markets within coupled power and gas networks. This framework enables effective and privacy-preserving coordination between hubs and the system operator while unlocking cost-effective flexibility within hubs. By enhancing system flexibility, reducing operational costs, and minimizing energy losses, the proposed approach addresses growing uncertainties in coupled power and gas networks and supports the reliable integration of renewable energy sources.

1.2. Related works

The increasing integration of flexibility markets in coupled power and gas networks has been a significant area of research, with a focus on the role of smart prosumers, such as energy hubs, smart buildings, Internet data centers, etc. Several studies have explored how multi-energy systems and demand-side flexibility can enhance energy efficiency, reduce operational costs, and improve grid stability. For instance, [13] presents a framework optimizing incentives for residential adoption of energy hubs, aiming for balanced economic benefits between utilities and consumers, demonstrating advantages such as peak load reduction and improved distribution system operations through Monte Carlo simulations. [14] outlines a method to enhance coordination between day-ahead scheduling and real-time dispatch in energy hubs, mitigating short-sighted decisions influenced by renewable variability, with performance close to optimal levels, comparable to predictive control methods. [5] proposes a risk management framework for electricity-gas systems, efficiently utilizing local energy hubs' flexibility to manage wind power variability, outperforming traditional approaches in computational efficiency. A key approach to managing flexibility in Peer-to-Peer (P2P) energy trading is proposed in [15], where prosumers optimize their energy consumption and trading within transactive power and gas systems. The model balances electricity and gas supply while enhancing system resilience through decentralized bi-level optimization. Similarly, [16] explores cost-sharing mechanisms in energy communities, demonstrating that smart prosumers can reduce their costs by actively participating in flexibility incentive programs. The integration of hydrogen storage as an additional flexibility source is discussed in [17], where Power-to-Gas (P2G) technology enables prosumers to optimize energy use and reduce dependence on centralized power generation. In the context of Virtual Power Plants (VPPs), [18] highlights how coordinated scheduling of power and gas markets can reduce price volatility while incentivizing prosumer participation in dual energy markets.

Energy flexibility is increasingly treated as a coordinated optimization problem spanning end-use control, network operation, and electrified mobility under uncertainty. Comfort-aware demand shaping is formulated for residential heating/ventilation with joint price-setpoint scheduling [19], complemented by sensor-driven rolling-horizon industrial load control under real-time tariffs [20] and wind-storage-demand response microgrid dispatch [21]. Communication, sensing, and cyber-physical enablement are captured through leader-follower incentives for telecom-assisted demand response [22], secure joint sensing-and-communication with optimized reflecting surfaces under imperfect channel knowledge [23], and measurement-based awareness in distribution grids via critical-node identification and voltage-sensitivity tracking [24,25]. Electric mobility flexibility is addressed through multi-timescale operation of solar-powered charging stations with storage [26] and strategic charging-infrastructure build decisions under platform competition [27]. At the system layer, scalability and decarbonization are pursued via accelerated network-constrained unit commitment [28] and low-carbon multi-energy dispatch coupling electricity, heat, gas, and hydrogen with power-to-gas, carbon capture, and hydrogen storage under interval uncertainty [29], supported by reliability/resilience studies on maintenance–replacement planning and fault performance enhancement [30,31]. Market participation realism and transition context are broadened by bounded rationality in local energy markets [32] and the coupling between green finance and green technology diffusion [33]. Adjacent transport and infrastructure analytics, accident reconstruction [34], mixed platoon control under delays [35], autonomous-driving adoption pathways [36], and real-time identification of vehicle-induced structural responses [37], reinforce that deployable flexibility frameworks must integrate optimization with data, communications, and human factors.

Decentralized energy trading has gained increasing attention, with [38] proposing a P2P-enabled system for microgrid communities. This model ensures transparent transactions while enhancing energy security and reducing reliance on centralized utilities. Similarly, [39] explores blockchain-enabled local electricity markets, leveraging heating system flexibility to optimize energy distribution among smart prosumers. In addition to energy trading, the role of energy hubs and rooftop solar prosumers in coordinated energy scheduling is studied in [40], where multi-energy optimization frameworks improve grid reliability and economic efficiency. A multi-agent deep reinforcement learning framework for energy trading and flexibility services is introduced in [41], demonstrating that AI-driven strategies enable prosumers to dynamically adjust consumption and generation based on real-time market conditions. [42] explores decentralized demand response for energy hubs, where integrated electricity and gas systems leverage linepack flexibility to optimize demand-side participation. Furthermore, [43] presents a bilevel energy-sharing framework that coordinates electricity and heating networks within integrated energy systems, emphasizing the role of flexible prosumers in reducing peak loads and enhancing system efficiency. Finally, [44] proposes a P2P framework for multi-energy microgrids in fully renewable integrated power and gas networks, employing P-robust stochastic optimization to manage uncertainties while facilitating decentralized electricity and gas trading.

Many studies have explored the utilization of demand-side flexibility resources, including energy storage systems, Electric Vehicle (EV) fleets, and flexible loads, within local markets. In this regard, [45] demonstrates that coordinated scheduling among energy hubs enhances system flexibility by leveraging storage systems and flexible loads to support system operators. Similarly, [46] proposes a two-phase optimization framework that integrates energy and ancillary service markets, achieving efficiency improvements and cost reductions through the coordination of conventional power sources, energy storage, EVs, and demand response aggregators. This approach yields a 10% reduction in thermal unit utilization and a 6.91% decrease in overall system costs. Additionally, [47] introduces a P2P trading framework for urban environments with EV charging stations, integrating transport and power distribution networks to reduce operational costs by 16.61% while maintaining network reliability standards. In Ref. [48], a robust MISOCP model with C&CG algorithm is presented for joint optimization of electricity and gas networks, incorporating DG, P2G, ESS, EVs, and DSM, achieving a 21% cost reduction.

A review of prior research underscores the widespread application of the ADMM in decentralized flexibility market coordination while highlighting the need for further refinement to enhance convergence speed and global optimality. Notable applications of ADMM include congestion and imbalance management in a 123-bus system [49], coordination between transmission and distribution systems to optimize flexibility utilization [50], facilitation of local flexibility markets in multi-Distribution System Operator (DSO) [51] and multi-microgrid [52] environments, development of a P2P architecture for energy and flexibility trading in distribution systems [53], and decentralized coordination of transmission and distribution flexibility markets [54]. Despite these advancements, further refinement is required to improve solution

Table 1
Comparison of the proposed approach with recent literature.

Ref	Studied markets		Security constraints		Energy Hubs			Demand-side Flexibility Resources			Privacy-preserving coordination among market agents	Enhanced ADMM-Based Coordination
	Energy	Flexibility	Power	Gas	Residential	Commercial	Industrial	Battery	V2G technology	IDR mechanism		
[13]	✓	×	✓	×	✓	×	×	✓	×	×	×	×
[14]	✓	×	✓	×	✓	×	×	✓	×	×	×	×
[5]	✓	×	✓	✓	✓	×	×	✓	×	×	×	×
[15]	✓	×	✓	×	×	×	×	✓	×	×	✓	×
[16]	✓	×	×	×	×	×	×	✓	×	×	×	×
[17]	✓	×	✓	✓	×	×	✓	✓	✓	×	✓	×
[18]	✓	×	✓	✓	×	×	×	×	×	×	×	×
[38]	✓	✓	✓	×	×	×	×	✓	✓	×	✓	✓
[39]	✓	✓	×	×	✓	×	×	×	×	×	✓	×
[40]	✓	✓	✓	✓	×	✓	×	✓	×	×	×	×
[41]	✓	✓	×	×	✓	×	×	✓	✓	×	✓	×
[42]	✓	✓	✓	✓	✓	×	×	✓	×	✓	✓	×
[43]	✓	×	✓	×	✓	×	×	×	×	×	✓	×
[44]	✓	×	✓	✓	×	×	×	✓	×	×	✓	×
[45]	✓	✓	×	×	✓	×	×	✓	✓	×	×	×
[46]	✓	✓	✓	×	×	×	×	✓	✓	×	×	×
[47]	✓	×	×	×	×	×	×	✓	✓	×	×	×
[48]	✓	×	✓	✓	×	×	×	✓	✓	×	×	×
[49]	✓	✓	✓	×	×	×	×	✓	×	✓	✓	×
[50]	×	✓	✓	×	×	×	×	✓	×	×	✓	✓
[51]	✓	✓	✓	×	×	×	×	✓	×	✓	✓	✓
[52]	✓	✓	✓	×	×	×	×	✓	✓	✓	✓	✓
[53]	✓	✓	✓	×	×	×	×	✓	×	✓	✓	×
[54]	×	✓	✓	×	×	×	×	×	×	×	✓	×
This Work	✓	✓	✓	✓	✓	✓	✓	✓	✓	✓	✓	✓

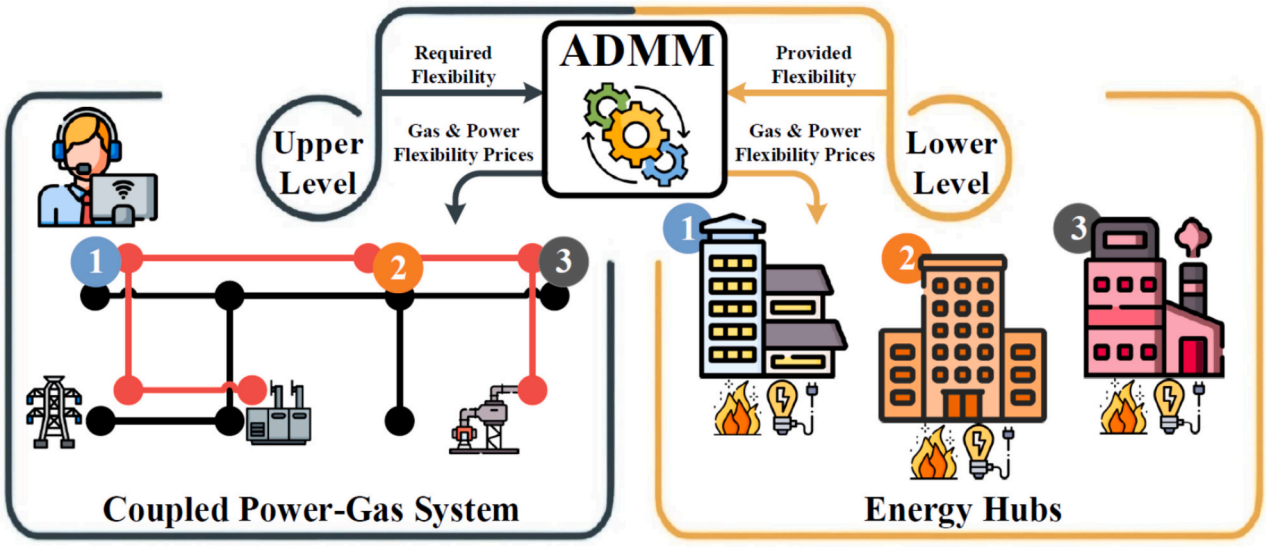

Fig. 1. ADMM-enabled model architecture.

accuracy and computational efficiency across various challenges.

1.3. Research gaps and contributions

Table 1 is introduced to highlight a detailed comparison of the proposed work with recent research. The literature extensively explores the role of smart prosumers in modernized flexibility markets. However, most studies have primarily focused on the flexibility of power networks while overlooking the integration of gas networks and their mutual interactions. Research that does consider both electricity and gas networks has predominantly examined energy markets, largely neglecting flexibility markets. Furthermore, while a limited number of studies have investigated flexibility markets in coupled electricity and gas networks, none have conducted a comprehensive analysis of the simultaneous operation of V2G technologies, IDR mechanisms, and diverse energy storage systems in terms of economic performance, flexibility enhancement, and system efficiency.

To partially address these research gaps, the authors previously introduced an ADMM-based model for integrating energy hubs into local flexibility markets in [55]. This model aimed to preserve market participants' privacy, enhance coordination speed, reduce daily operational costs, and maximize the utilization of flexible capacities from advanced demand-side technologies. However, the model did not incorporate the gas network, its real-time energy imbalances, or its interactions with the power network. Additionally, the energy hubs were assumed to follow a uniform structural framework, preventing the analysis of diverse real-world hub configurations with varying operational characteristics.

Building on prior research and addressing these limitations, this paper presents a comprehensive model for the decentralized coordination of energy hubs in coupled electricity and gas networks. The proposed model optimizes the deployment of flexible technologies within energy hubs to improve economic performance, enhance system flexibility, and increase operational efficiency. This model explicitly accounts for real-time energy imbalances in both electricity and gas networks, capturing their interdependencies. Moreover, it accommodates energy hubs with distinct residential, commercial, and industrial configurations, allowing for a more realistic representation of real-world systems. Furthermore, the ADMM algorithm introduced in [55] has been enhanced with a logarithmic coefficient-based technique for dynamic error updating, significantly improving the convergence speed of the agents. The main contributions of this model are outlined below:

- Proposing a bi-level optimization model in which the coupled power-gas system operator is embedded at the upper level, while residential, commercial, and industrial energy hubs operate at the lower level. This setup enables the system operator to effectively manage flexibility requirements, mitigating generation-consumption imbalances within the coupled power-gas system by leveraging the cost-effective flexibility of advanced demand-side technologies within energy hubs. Leveraging the full potential of energy hubs, the proposed model reduces reliance on external networks, minimizes power losses, lowers system operator costs, and ensures the economic viability of energy hubs in local flexibility markets.
- Presenting a novel adaptive version of ADMM for the decentralized coordination of energy hubs and the coupled power-gas system operator, incorporating a logarithmic coefficient-based technique for dynamic error updating. This enhanced version achieves significantly faster convergence compared to both the standard ADMM and the version presented in [55]. Moreover, it ensures the global optimality of market optimization while preserving the confidentiality of energy hubs' internal information by minimizing data exchange between agents and the system operator.
- Developing an energy management mechanism for residential, commercial, and industrial energy hubs that optimally integrates their electrical, thermal, and cooling converters with advanced demand-side technologies, including V2G, IDR mechanisms, and electrical, thermal, and cooling storage systems. The proposed mechanism unlocks the full flexibility potential of energy hubs, optimizing their service provision to intra-day flexibility markets and increasing their profitability.

2. Proposed bi-level model

Fig. 1 illustrates the structure of the proposed model, designed to unlock the maximum flexibility potential of smart prosumers, particularly residential, commercial, and industrial energy hubs, within intra-day flexibility markets in modern coupled power-gas systems. The flexibility market analyzed in this study is structured to address intra-

hour generation-consumption imbalances in both power and gas networks. It facilitates real-time coordination between network operators and market participants, leveraging distributed flexibility resources to enhance operational reliability and efficiency. The model comprises two levels: the upper level, where the coupled power-gas system operator performs intra-day operational planning of its area, and the lower level, where energy hubs optimize their flexibility provision. At the upper level, the system operator eliminates inter-hourly generation-consumption imbalances in the power and gas networks while ensuring compliance with all security constraints governing energy flows. Upon solving this optimization stage, the operator determines the operation schedules for dispatchable generation units and electrical and gas storage systems, aligning them with inter-hour fluctuations. Additionally, it specifies the required upward and downward flexibility capacities at the coupling points connecting external networks and downstream hubs, for both electricity and gas. At the lower level, each energy hub employs an energy management mechanism to optimize the flexibility of its internal technologies. After solving this stage, hub operators establish optimal schedules for all internal technologies and loads while reporting their available upward and downward flexibility capacities to the system operator.

An enhanced adaptive ADMM algorithm is introduced to ensure decentralized coordination between the system operator and energy hubs. This distributed optimization-based mechanism guarantees convergence to the global optimum while preserving participant privacy by restricting shared information to essential service exchange parameters. The mechanism links the final pricing of electricity and gas flexibility services to mutual interactions between hubs and the system operator, as well as network energy flow constraints, ensuring a competitive market environment.

3. Mathematical formulation

This section presents a Mixed-Integer Linear Programming (MILP) formulation for modeling the first and second levels and a Mixed-Integer Quadratically Constrained Programming (MIQCP) formulation for the proposed adaptive ADMM algorithm. The energy market is assumed to have been settled on the previous day, with its results available to the system operator. To account for intra-hourly generation-consumption fluctuations required for the operation of the intra-day flexibility market, white noise is introduced to the load demand, PV power output, and wind power generation. This noise is modeled using Gaussian, Beta, and Weibull Probability Distribution Functions (PDFs) for load demand, PV generation, and wind power, respectively, with parameters estimated using standard statistical methods: Gaussian parameters (μ, σ) from historical load data, Beta parameters (α, β) from normalized solar irradiance using method-of-moments, and Weibull parameters (k, λ) from wind speed data using maximum likelihood estimation.

3.1. Upper-level scheduling

Eq. (1) defines the objective function of the coupled power-gas system operator, formulated to minimize costs associated with system flexibility requirements. This function incorporates the procurement of flexibility services from energy hubs, external networks, dispatchable units, and electrical and gas storage systems. The costs of services procured from external networks, dispatchable generation units, and storage systems are predefined parameters, whereas the costs of services obtained from energy hubs are iteratively updated based on the convergence of the proposed ADMM. Initially, $\lambda_{h,t}^{P,Hub}$ and $\lambda_{h,t}^{G,Hub}$ are treated as inputs during the first ADMM iteration but are subsequently adjusted based on ADMM penalties and discrepancies in planning between the system operator and energy hubs. A detailed discussion of this process is provided in Subsection C.

$$\begin{aligned} F^{SO} = & \sum_h \sum_t \left[\lambda_{h,t}^{P,Hub} \left(P_{h,t}^{Hub,U} + P_{h,t}^{Hub,D} \right) \Delta t + \lambda_{h,t}^{G,Hub} \left(G_{h,t}^{Hub,U} + G_{h,t}^{Hub,D} \right) \right] \\ & + \sum_t \left[\pi_t^{P,EN} \left(P_t^{EN,U} + P_t^{EN,D} \right) \Delta t + \pi_t^{G,EN} \left(G_t^{EN,U} + G_t^{EN,D} \right) \right] \\ & + \sum_g \sum_t \left[\pi_g^{GU} \left(P_{g,t}^{GU,U} + P_{g,t}^{GU,D} \right) \Delta t \right] \\ & + \sum_t \left(\sum_{es} \left[\pi_{es}^{ES} \left(P_{es,t}^{ES,U} + P_{es,t}^{ES,D} \right) \Delta t \right] + \sum_{gs} \left[\pi_{gs}^{GS} \left(G_{gs,t}^{GS,U} + G_{gs,t}^{GS,D} \right) \right] \right) \end{aligned} \tag{1}$$

The system operator employs a linearized AC power flow model to manage energy transactions within the power network, as described in (a1)-(a8) [15]. Equation (a1) defines the active power flow of line l based on voltage magnitude and angle at both terminals, while (a2) provides a similar formulation for reactive power [46]. Line losses, incorporating active/reactive power and line resistance, are computed in (a3). To enhance computational tractability, a piecewise linearization technique is employed to approximate the quadratic terms associated with active and reactive power flows. Voltage magnitude and angle constraints for network buses are enforced through (a4) and (a5), respectively. Equation (a6) restricts power flows to line capacities (S_l^F), whereas (a7) and (a8) ensure active and reactive power balance at each bus. Letters with a bar denote variables predetermined in the prior day's energy market, whereas those without a bar correspond to the current day's flexibility market. Parameter $\tau_{i,l}^F$ determines the direction of power flow, taking values of 1, 0, or − 1, depending on the network topology. Parameters $\delta_{i,t}^D$, $\delta_{s,t}^{PV}$, and $\delta_{w,t}^{WT}$ are respectively generated using Gaussian, Beta, and Weibull PDFs, applying white noise to the outcomes of the prior day's settled energy market, specifically load demand, PV power, and wind power.

$$\frac{P_{l,t}^F}{S^B} = G_l \left(v_{i,t} - v_{j,t} \right) + B_l \left(\theta_{i,t} - \theta_{j,t} \right) \tag{a1}$$

$$\frac{Q_{l,t}^F}{S^B} = B_l \left(v_{i,t} - v_{j,t} \right) - G_l \left(\theta_{i,t} - \theta_{j,t} \right) \tag{a2}$$

$$P_{l,t}^L = \frac{R_l \left[\left(P_{l,t}^F \right)^2 + \left(Q_{l,t}^F \right)^2 \right]}{S^B} \tag{a3}$$

$$v_i^{Min} \le v_{i,t} \le v_i^{Max} \tag{a4}$$

$$\theta_i^{Min} \le \theta_{i,t} \le \theta_i^{Max} \tag{a5}$$

$$\left(P_{l,t}^F \right)^2 + \left(Q_{l,t}^F \right)^2 \le \left(S_l^F \right)^2 \tag{a6}$$

$$\begin{aligned} & \left(\overline{P}_t^{EN} + P_t^{EN,U} - P_t^{EN,D} \right) \Big|_{i=1} + \sum_{g \in \Pi_i^g} \left(\overline{P}_{g,t}^{GU} + P_{g,t}^{GU,U} - P_{g,t}^{GU,D} \right) \\ & + \sum_{s \in \Pi_i^s} \left(\delta_{s,t}^{PV} \overline{P}_{s,t}^{Solar} \right) + \sum_{w \in \Pi_i^w} \left(\delta_{w,t}^{WT} \overline{P}_{w,t}^{Wind} \right) \\ & + \sum_{es \in \Pi_i^{es}} \left(\overline{P}_{es,t}^{ES} + P_{es,t}^{ES,U} - P_{es,t}^{ES,D} \right) = \delta_{i,t}^D \overline{P}_{i,t}^D \\ & + \sum_{h \in \Pi_i^h} \left(\overline{P}_{h,t}^{Hub} - P_{h,t}^{Hub,U} + P_{h,t}^{Hub,D} \right) + \sum_l \left(\tau_{i,l}^F P_{l,t}^F + \left| \tau_{i,l}^F \right| \frac{P_{l,t}^L}{2} \right) \end{aligned} \tag{a7}$$

$$Q_t^{EN} \Big|_{i=1} + \sum_{g \in \Pi_i^g} Q_{g,t}^{GU} + = \sum_l \left(\tau_{i,l}^F Q_{l,t}^F \right) + \delta_{i,t}^D Q_{i,t}^D + \sum_{h \in \Pi_i^h} \left[\varpi_h^{Hub} \left(\overline{P}_{h,t}^{Hub} - P_{h,t}^{Hub,U} + P_{h,t}^{Hub,D} \right) \right] \tag{a8}$$

The operational constraints of the gas network are detailed in (b1)-(b3). Equation (b1) imposes bounds on nodal gas pressure to maintain it within permissible limits. Equation (b2) models gas flow in each

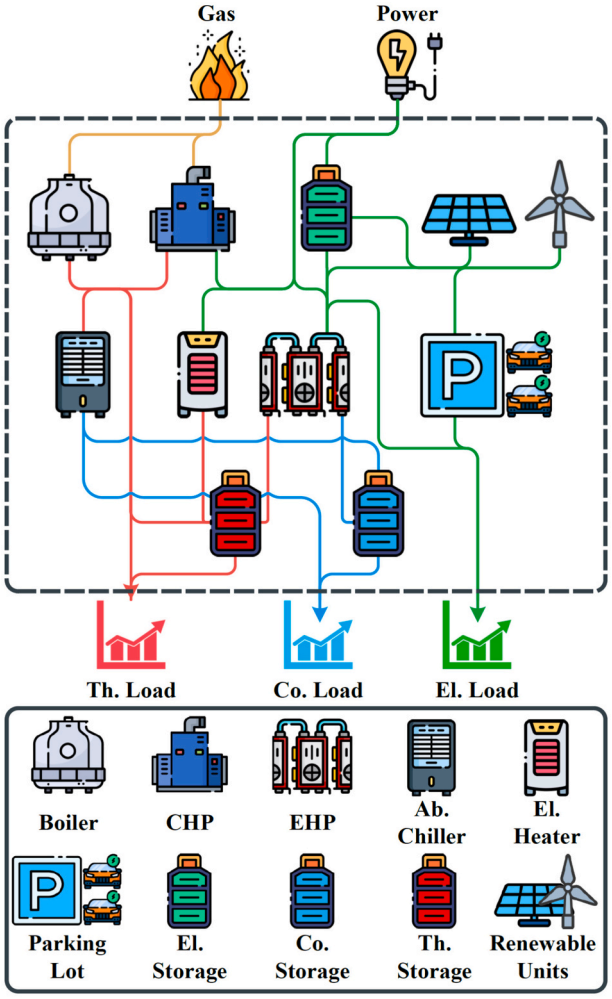

Fig. 2. Conceptual representation of energy hubs.

pipeline and is linearized using a 10-segment piecewise linear approximation to enhance computational efficiency. Following the validation approach in [56], this piecewise linearization maintains high accuracy with errors typically below 1% for distribution network operating conditions while enabling efficient MILP formulation instead of computationally expensive nonlinear programming. The parameters $Pr_{i,t}$ and $Pr_{j,t}$ denote the inlet and outlet pressures of the pipeline, respectively, while the constant ϑ_i^p encapsulates the pipeline's physical characteristics. (b3) ensures nodal equilibrium by enforcing the balance between total gas supply and demand across all nodes. Factor $\delta_{i,t}^D$ applies white noise to the day-ahead energy market's gas demand ($\overline{G}_{i,t}^D$) to simulate intraday fluctuations. The upward and downward capacities required to manage these fluctuations can be supplied by energy hubs, the external gas network, dispatchable generation units, and gas storage systems.

$$Pr_i^{Min} \le Pr_{i,t} \le Pr_i^{Max} \tag{b1}$$

$$G_{l,t}^F \left| G_{l,t}^F \right| = \left(\vartheta_l^p\right)^2 \left[\left(Pr_{i,t}\right)^2 - \left(Pr_{j,t}\right)^2 \right] \tag{b2}$$

$$\begin{aligned} &\left(\overline{G}_t^{EN} + G_t^{EN,U} - G_t^{EN,D}\right)\Big|_{i=1} + \sum_{gs \in \Pi_i^{gs}} \left(\overline{G}_{gs,t}^{GS} + G_{gs,t}^{GS,U} - G_{gs,t}^{GS,D}\right) = \\ &\sum_l \left(\tau_{i,l}^F G_{l,t}^F\right) + \delta_{i,t}^D \overline{G}_{i,t}^D + \sum_{g \in \Pi_i^g} \left(\overline{G}_{g,t}^{GU} - G_{g,t}^{GU,U} + G_{g,t}^{GU,D}\right) \end{aligned} \tag{b3}$$

The power-gas system components incorporate dispatchable generating units, wind units, PV units, electricity and gas storage systems, and gas booster compressors. The active power output of dispatchable units is determined using (c1), where M^G and LHV^G denote the fuel mass flow rate and lower heating value, respectively, whereas $G_{g,t}^{GU}$ and η_g^{GU} represent the gas flow rate and efficiency coefficient. ϕ is a factor of 3.6 used to ensure unit consistency. Constraints on the active and reactive power setpoints of dispatchable units in the intra-day flexibility market are formulated in (c2) and (c3), considering unit capacities and operational setpoints from the previous day's energy market outcomes. The binary variable $I_{g,t}^{GU}$ is a binary variable that indicates whether dispatchable unit g is on or off at time t. The wind power generation model in (c4) describes output as a segmented function of the hourly wind speed (S_t), distinguishing three operational phases: (i) no generation when wind speed is below the cut-in threshold (S_{ci}), (ii) a gradual increase in power as wind speed rises from S_{ci} to the rated value S_r, and (iii) full power output when wind speed falls within the rated and cut-out limits (S_{co}). The PV generation framework in (c5) accounts for key parameters, including hourly solar irradiance (SI_t), reference irradiance (SI^R), panel efficiency (η_s^{PV}), and maximum installed capacity ($P_s^{PV,Max}$). Gas compressors, as defined in (c6), function to elevate gas pressure by compressing the incoming flow before network injection.

$$P_{g,t}^{GU} = \frac{M^G LHV^G \eta_g^{GU} G_{g,t}^{GU}}{\phi} \tag{c1}$$

$$P_g^{GU,Min} I_{g,t}^{GU} \le P_{g,t}^{GU} \le P_g^{GU,Max} I_{g,t}^{GU} \tag{c2}$$

$$Q_g^{GU,Min} I_{g,t}^{GU} \le Q_{g,t}^{GU} \le Q_g^{GU,Max} I_{g,t}^{GU} \tag{c3}$$

$$P_{w,t}^{WT} = \begin{cases} 0 & , \ S_t < S_{ci} \ \text{ Or } \ S_t \ge S_{co} \\ P_w^{WT,Max} \dfrac{S_t - S_{ci}}{S_r - S_{ci}} & , \ S_{ci} \le S_t < S_r \\ P_w^{WT,Max} & , \ S_r \le S_t < S_{co} \end{cases} \tag{c4}$$

$$P_{s,t}^{PV} = \eta_s^{PV} \frac{SI_t}{SI^R} P_s^{PV,Max} \tag{c5}$$

$$Pr_{j,t} = \Delta^C Pr_{i,t} \tag{c6}$$

The operational modeling of electrical storage systems is defined in (d1)-(d6). In (d1) and (d2), the charging and discharging power levels, $P_{es,t}^{Ch}$ and $P_{es,t}^{Dis}$, are constrained by their respective maximum capacities and predefined setpoints obtained in the previous day's energy market. The charging status of the storage system is determined by the binary variable $I_{es,t}^{Ch}$. The energy balance equation (d3) updates the stored energy level based on the preceding state and the net energy exchange. Initial and final storage levels are predefined in (d4), while constraint (d5) maintains the stored energy within permissible limits, bounded by $E_{es}^{ES,Min}$ and $E_{es}^{ES,Max}$. Equation (d6) computes the storage system's net exchange ($P_{es,t}^{ES}$) with the grid at time t, considering charging and discharging power.

$$0 \le P_{es,t}^{Ch} \le P_{es}^{Ch,Max} I_{es,t}^{Ch} \tag{d1}$$

$$0 \le P_{es,t}^{Dis} \le P_{es}^{Dis,Max} \left(1 - I_{es,t}^{Ch}\right) \tag{d2}$$

$$E_{es,t}^{ES} = E_{es,t-1}^{ES} + \eta_{es}^{Ch} P_{es,t}^{Ch} \Delta t - \frac{P_{es,t}^{Dis}}{\eta_{es}^{Dis}} \Delta t \tag{d3}$$

$$E_{es,t=0}^{ES} = E_{es,t=T}^{ES} = E_{es}^{ES,0} \tag{d4}$$

$$E_{es}^{ES,Min} \le E_{es,t}^{ES} \le E_{es}^{ES,Max} \tag{d5}$$

$$P_{es,t}^{ES} = P_{es,t}^{Dis} - P_{es,t}^{Ch} \tag{d6}$$

The operational modeling of gas storage systems follows a similar

structure and is defined in (e1)-(e5). Constraint (e1) updates the gas storage volume based on the previous state and net gas injection/withdrawal, where $\eta_g$represents the storage efficiency. Equation (e2) limits the injection and extraction rates to their maximum capacities. Initial and final storage volumes are set equal in (e3), while (e4) maintains the stored gas volume within permissible limits. Equation (e5) computes the net gas exchange with the network.

$$V_{g_s,t} = V_{g_s,t-1} + \left(\eta_{g_s} G^{in}_{g_s,t} - \frac{1}{\eta_{g_s}} G^{out}_{g_s,t}\right)\Delta t \tag{e1}$$

$$\begin{aligned} 0 \le G^{in}_{g_s,t} \le G^{max,in}_{g_s} \\ 0 \le G^{out}_{g_s,t} \le G^{max,out}_{g_s} \end{aligned} \tag{e2}$$

$$V_{g_s,0} = V_{g_s,T} \tag{e3}$$

$$V^{min}_{g_s} \le V_{g_s,t} \le V^{max}_{g_s} \tag{e4}$$

$$G^{GS,U}_{g_s,t} - G^{GS,D}_{g_s,t} = G^{out}_{g_s,t} - G^{in}_{g_s,t} \tag{e5}$$

Gas storage systems enhance flexibility by providing bidirectional services by injecting gas during supply shortages and extracting during surplus conditions, unlike dispatchable units constrained to their power generation schedules. This decouples gas supply from instantaneous demand, smoothing demand variations and reducing reliance on external networks. Additionally, gas networks possess inherent linepack flexibility, where gas volume stored within pipelines can be adjusted through pressure variations within limits (b1)-(b2). As demonstrated in [42], linepack provides rapid intra-hour balancing, while dedicated gas storage (e1)-(e5) addresses sustained imbalances, creating a two-tier flexibility framework essential for managing renewable intermittency in coupled power-gas systems.

3.2. Lower-level scheduling

The lower-level model incorporates an energy management mechanism that enables diverse energy hubs to maximize their participation in the intra-day flexibility market. As depicted in Fig. 2, these hubs can exchange bidirectional power and unidirectional gas with their respective networks. They must supply electrical, thermal, and cooling loads while implementing an IDR mechanism. Energy hubs differ in component configurations, capacity, and load profile, with each hub integrating a specific subset of available technologies based on its internal design. Depending on their setup, energy hubs can meet electrical loads through grid exchanges, Combined Heat and Power (CHP) systems, PV units, wind turbines, and electrical storage discharge. Thermal loads may be supplied by CHP systems, boilers, Electric Heat Pumps (EHPs), electric heaters, and thermal storage discharge, while cooling loads can be met using absorption chillers, EHPs, and cooling storage discharge. Additionally, energy hubs incorporate parking lots for EV fleets, enabling V2G services.

The lower-level objective function, defined in (2), maximizes the energy hubs' profit in the intra-day flexibility market. This function comprises two components: the first accounts for profits from providing flexibility services to the power network, while the second pertains to services for the gas network. Each energy hub optimizes this objective independently, ensuring operator privacy. $I^{P,U}_t$ and $I^{P,D}_t$ are parameters that define the system operator's upward and downward flexibility needs in the power network at any time t. These parameters are determined at the end of the upper-level optimization and communicated to the hubs. If upward services are required at t, $I^{P,U}_t = 1$, and vice versa. Note that $I^{P,U}_t$ and $I^{P,D}_t$ are mutually exclusive. Similarly, $I^{G,U}_t$ and $I^{G,D}_t$ serve the same role for the gas network.

The balance constraints for electrical, thermal, cooling, and gas loads are formulated in (f1)-(f4), respectively. These constraints comprehensively include all components, with each energy hub excluding variables corresponding to non-existent components based on its configuration. Additionally, the balance constraints incorporate variables required for implementing the IDR mechanism across all three load types, enabling hub operators to adjust their loads accordingly. Equations (f5) and (f6) restrict load shift-up and shift-down to a percentage of their maximum values, respectively. Binary variables $I^{P/H/C,+}_{h,t}$ and $I^{P/H/C,-}_{h,t}$ activate shift-up and shift-down operations, with their mutual exclusivity enforced in constraint (e7).

$$\begin{aligned} F^{Hub}_h = \sum_t \left[\lambda^{P,Hub}_{h,t}\left(P^{Hub,U}_{h,t} I^{P,U}_t + P^{Hub,D}_{h,t} I^{P,D}_t\right)\Delta t\right] \\ + \sum_t \left[\lambda^{G,Hub}_{h,t}\left(G^{Hub,U}_{h,t} I^{G,U}_t + G^{Hub,D}_{h,t} I^{G,D}_t\right)\right] \end{aligned} \tag{2}$$

$$\begin{aligned} \overline{P}^{Hub}_{h,t} - P^{Hub,U}_{h,t} + P^{Hub,D}_{h,t} = L^{P}_{h,t} + L^{P,+}_{h,t} + P^{EH}_{h,t} + P^{EHP}_{h,t} + P^{Ch}_{h,t} + \sum_{ev \in \Pi^{ev}_h} P^{Ch}_{ev,t} - L^{P,-}_{h,t} \\ - P^{CHP}_{h,t} - P^{PV}_{h,t} - P^{WT}_{h,t} - P^{Dis}_{h,t} - \sum_{ev \in \Pi^{ev}_h} P^{Dis}_{ev,t} \end{aligned} \tag{f1}$$

$$H^{CHP}_{h,t} + H^{Boiler}_{h,t} + H^{EH}_{h,t} + H^{Dis}_{h,t} + H^{EHP}_{h,t} + L^{H,-}_{h,t} = L^{H}_{h,t} + L^{H,+}_{h,t} + H^{Ch}_{h,t} + H^{AC}_{h,t} \tag{f2}$$

$$C^{AC}_{h,t} + C^{EHP}_{h,t} + C^{Dis}_{h,t} + L^{C,-}_{h,t} = L^{C}_{h,t} + L^{C,+}_{h,t} + C^{Ch}_{h,t} \tag{f3}$$

$$\overline{G}^{Hub}_{h,t} - G^{Hub,U}_{h,t} + G^{Hub,D}_{h,t} = G^{CHP}_{h,t} + G^{Boiler}_{h,t} \tag{f4}$$

$$0 \le L^{P/H/C,+}_{h,t} \le \alpha^{P/H/C}_h L^{P/H/C}_{h,t} I^{P/H/C,+}_{h,t} \tag{f5}$$

$$0 \le L^{P/H/C,-}_{h,t} \le \alpha^{P/H/C}_h L^{P/H/C}_{h,t} I^{P/H/C,-}_{h,t} \tag{f6}$$

$$I^{P/H/C,+}_{h,t} + I^{P/H/C,-}_{h,t} \le 1 \tag{f7}$$

The formulation of electrical, thermal, and cooling energy storage systems within hubs follows the approach used for storage systems in the upper level. Other hub components are represented by constraints (fg1)-(g13). Note that the internal energy flow between components follows the structure depicted in Fig. 2. The operational constraints of CHP systems, formulated in (g1)-(g6), define their feasible operating region as a trapezoid with vertices A, B, C, and D. Constraint (g1) ensures the operating point remains below line AB, while (g2) enforces it above BC, and (g3) maintains operation above CD. The binary variable $I^{CHP}_{h,t}$ indicates the unit's operational status. Constraints (g4) and (g5) define the permissible heat and power generation limits. Equation (g6) models the CHP unit's gas demand, incorporating electrical ($P^{CHP}_{h,t}$) and thermal ($H^{CHP}_{h,t}$) energy outputs. These outputs are scaled by efficiency factors η^{gp}_h and η^{gh}_h and adjusted using the gas's lower heating value LHV^G and molar mass (M^G). A conversion factor of 3.6 (ϕ) ensures unit compatibility. Similarly, the boiler's gas consumption is determined in (g7), based on its operating state ($H^{Boiler}_{h,t}$). The EHP operation follows (g8), linking heating and cooling outputs to power input ($P^{EHP}_{h,t}$) and respective efficiencies (η^{eh}_h and η^{ec}_h). Equations (g9) and (g10) prevent simultaneous heating and cooling production, controlled by the binary variable $I^{EHP}_{h,t}$, which determines the EHP's mode. Absorption chillers supply cooling as per (g11), while electric heaters generate thermal power under (g12). A general capacity constraint (g13) ensures that all hub components operate within their respective maximum limits.

$$P^{CHP}_{h,t} + \frac{P^A_h - P^B_h}{H^A_h - H^B_h}\left(H^{CHP}_{h,t} - H^A_h\right) \le P^A_h \tag{g1}$$

$$P^{CHP}_{h,t} + \frac{P^B_h - P^C_h}{H^B_h - H^C_h}\left(H^{CHP}_{h,t} - H^B_h\right) \ge P^B_h - \left(1 - I^{CHP}_{h,t}\right)M \tag{g2}$$

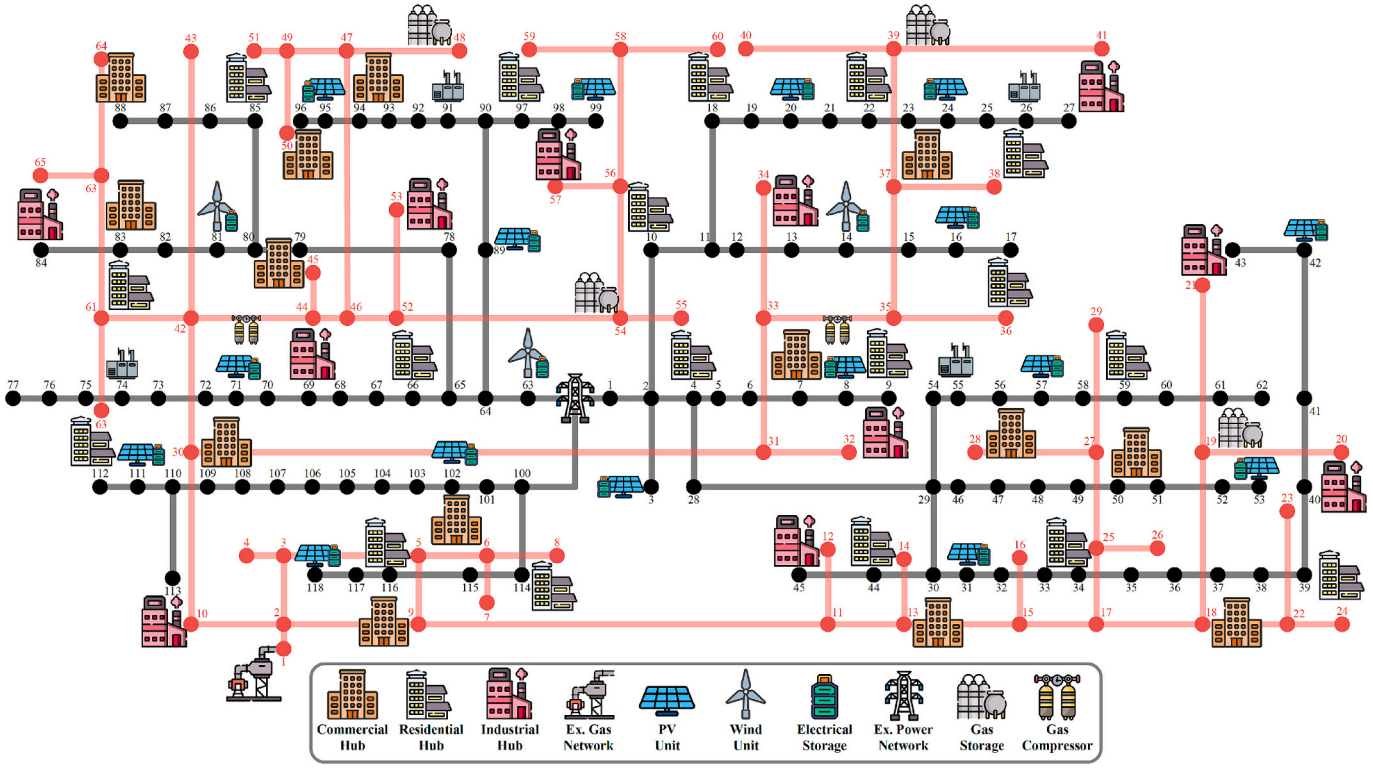

Fig. 3. Coupled power-gas system under analysis.

Table 2
Structural configuration of the case studies.

Case	Network Storage Systems	Energy Hub Technologies		
		IDR Mechanisms	Storage Systems	V2G Services
1	×	×	×	×
2	✓	×	×	×
3	✓	✓	×	×
4	✓	✓	✓	×
5	✓	✓	✓	✓

Table 3
Numerical outcomes achieved for Cases 1–5.

Case	System Operator's Flexibility Market Expenses ($)			
	System Components	External Networks	Energy Hubs	Sum.
1	2787.37	43,681.81	0	46,469.18
2	3749.77	38,833.41	0	42,583.19
3	3749.77	32,292.47	2878.01	38,920.26
4	3749.77	30,198.52	3464.32	37,412.61
5	3749.77	26,765.41	3835.24	34,350.43

$$P_{h,t}^{CHP}+\frac{P_h^C-P_h^D}{H_h^C-H_h^D}\left(H_{h,t}^{CHP}-H_h^C\right)\geq P_h^C-\left(1-I_{h,t}^{CHP}\right)M \tag{g3}$$

$$0\leq H_{h,t}^{CHP}\leq H_h^B I_{h,t}^{CHP} \tag{g4}$$

$$P_h^C I_{h,t}^{CHP}\leq P_{h,t}^{CHP}\leq P_h^A I_{h,t}^{CHP} \tag{g5}$$

$$G_{h,t}^{CHP}=\frac{\phi}{M^G LHV^G}\left(\frac{P_{h,t}^{CHP}}{\eta_h^{gp}}+\frac{H_{h,t}^{CHP}}{\eta_h^{gh}}\right) \tag{g6}$$

$$G_{h,t}^{Boiler}=\frac{\phi H_{h,t}^{Boiler}}{M^G LHV^G \eta_h^{Boiler}} \tag{g7}$$

$$P_{h,t}^{EHP}=\frac{C_{h,t}^{EHP}}{\eta_h^{ec}}+\frac{H_{h,t}^{EHP}}{\eta_h^{eh}} \tag{g8}$$

$$H_{h,t}^{EHP}\leq I_{h,t}^{EHP}M \tag{g9}$$

$$C_{h,t}^{EHP}\leq\left(1-I_{h,t}^{EHP}\right)M \tag{g10}$$

$$C_{h,t}^{AC}=\eta_h^{hc}H_{h,t}^{AC} \tag{g11}$$

$$H_{h,t}^{EH}=\eta_h^{eh}P_{h,t}^{EH} \tag{g12}$$

$$\begin{cases} H_{h,t}^{Boiler}\leq H_h^{Boiler,Max} \\ C_{h,t}^{AC}\leq C_h^{AC,Max} \\ P_{h,t}^{EH}\leq P_h^{EH,Max} \\ P_{h,t}^{EHP}\leq H_h^{EHP,Max} \end{cases} \tag{g13}$$

Equations (h1)-(h6) define the operation of V2G-enabled parking lots at energy hubs, where charging and discharging of vehicle batteries are managed based on market signals while respecting vehicle availability constraints. Equation (h1) tracks the EV battery's energy level on an hourly basis, incorporating previous energy levels and current charging or discharging. Equations (h2) and (h3) define the maximum charge and discharge rates, while (h4) limits the battery's energy capacity. Parameter $u_{ev,t}^{P}$ is nonzero only when vehicles are present, ensuring that charging and discharging occur only while vehicles are in the parking lot. Equation (h5) sets the EV battery energy level upon arrival, and (h6) ensures it meets a minimum threshold at departure.

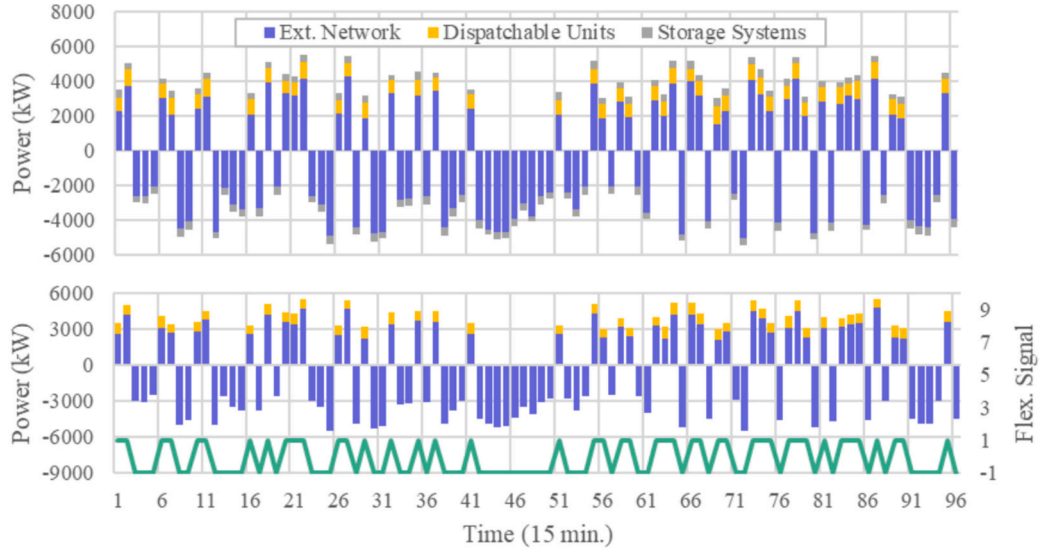

Fig. 4. Flexibility providers in the power network.

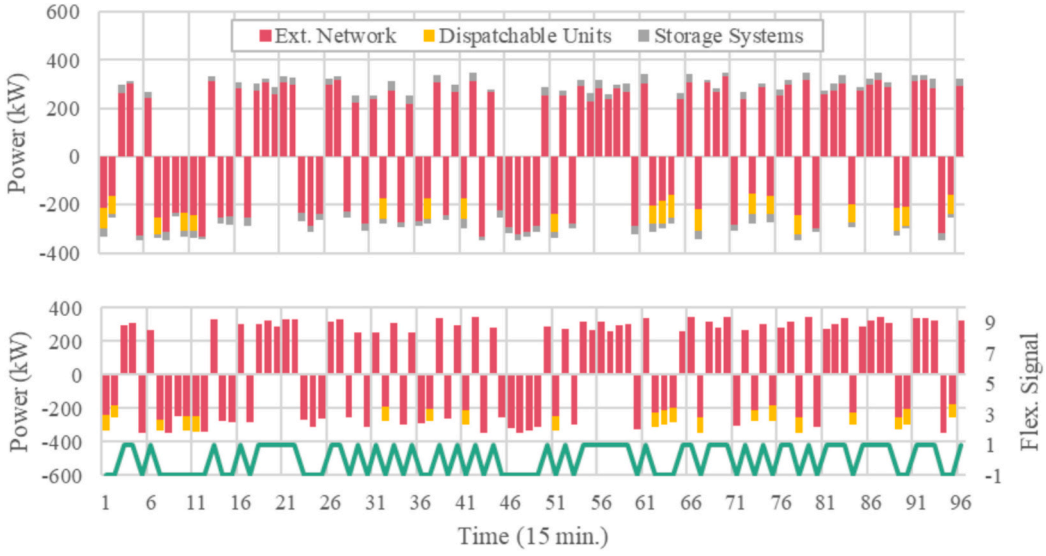

Fig. 5. Flexibility providers in the gas network.

$$E^{EV}_{ev,t} = E^{EV}_{ev,t-1} + P^{Ch}_{ev,t}\eta^{Ch}_{ev}\Delta t - \frac{P^{Dis}_{ev,t}}{\eta^{Dis}_{ev}}\Delta t \tag{h1}$$

$$0 \le P^{Ch}_{ev,t} \le P^{Ch,Max}_{ev} I^{Ch}_{ev,t} u^{P}_{ev,t} \tag{h2}$$

$$0 \le P^{Dis}_{ev,t} \le P^{Dis,Max}_{ev}\left(1 - I^{Ch}_{ev,t}\right) u^{P}_{ev,t} \tag{h3}$$

$$E^{EV,Min}_{ev} \le E^{EV}_{ev,t} \le E^{EV,Max}_{ev} \tag{h4}$$

$$E^{EV}_{ev,t=T^{u}} = E^{EV,Ar}_{ev} \tag{h5}$$

$$E^{EV}_{ev,t=T^{d}} \ge E^{EV,Dp}_{ev} \tag{h6}$$

3.3. Linking upper and lower levels

This work introduces an enhanced ADMM framework designed to facilitate the coordination between upper- and lower-level optimization agents in the intra-day flexibility market. The proposed approach enables the upper-level agent (e.g., a system operator) to determine the necessary flexibility services, while the lower-level agents (e.g., energy hubs) independently specify their service provisions. To preserve local confidentiality, only coupling variables associated with upward and downward flexibility contributions are exchanged between energy hubs and the system operator. A key distinction from conventional ADMM lies in the dynamic adaptation of penalty parameters. Unlike traditional methods that use static penalty coefficients, the proposed approach continuously updates these terms throughout the iterative process, enhancing convergence speed and stability.

The proposed ADMM framework guarantees global optimality through its convex problem structure and convergence properties. Both the upper-level (system operator) and lower-level (energy hubs) are formulated as MILP problems with linear constraints and convex objectives. For such problems, ADMM provably converges to the global optimum when augmented Lagrangian penalty terms are appropriately selected. Convergence is verified through primal residuals (measuring coupling variable agreement between agents) and dual residuals (tracking flexibility price stabilization). When both metrics fall below the threshold ($\sum PR + \sum DR \le 0.001$), the algorithm reaches a state

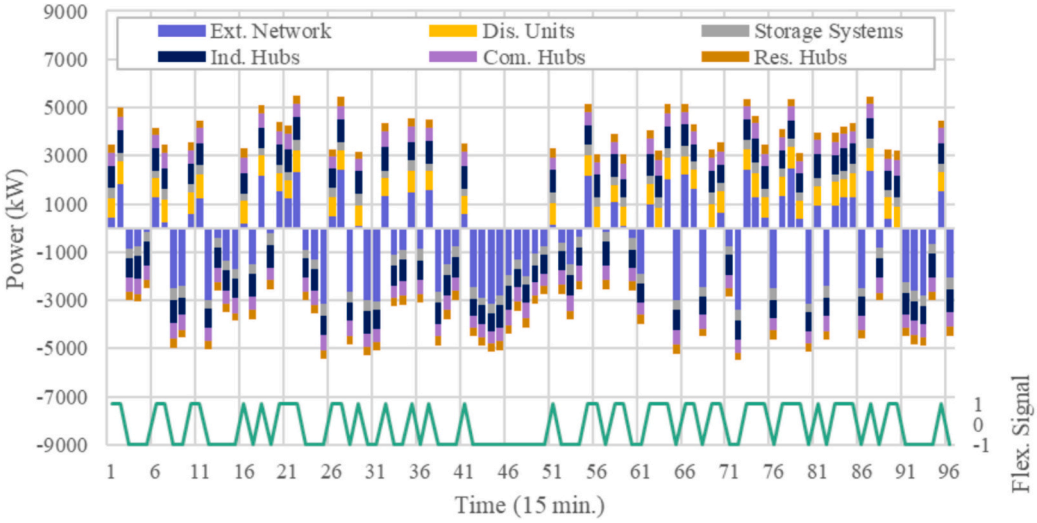

Fig. 6. Flexibility providers in the power network.

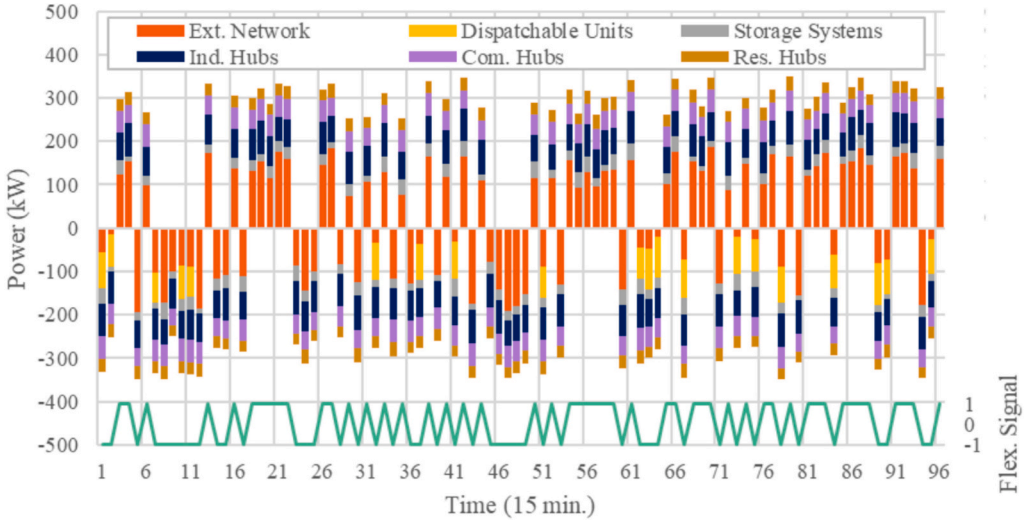

Fig. 7. Flexibility providers in the gas network.

where no agent can unilaterally improve its objective without violating system constraints, confirming global optimality. The adaptive penalty coefficient adjustment accelerates convergence without compromising optimality, as evidenced in Fig. 12, where all ADMM variants converge to identical objective values.

The implementation steps are outlined in Algorithm 1. In lines 1–4, the initial settings of the proposed ADMM framework are established, including the initialization of exchange prices for electricity and gas flexibility services in the first iteration. These prices are dynamically updated in subsequent iterations based on deviations between the upper- and lower-level solutions. Following this, the upper- and lower-level objective functions are reformulated (lines 5 and 6) by integrating ADMM penalty terms, denoted as $\left\|P_{h,t}^{Hub}-\widetilde{P}_{h,t}^{Hub}\right\|_2^2$ and $\left\|G_{h,t}^{Hub}-\widetilde{G}_{h,t}^{Hub}\right\|_2^2$, which are weighted by dynamically updated coefficients $\frac{\rho_h^P}{2}$ and $\frac{\rho_h^G}{2}$. Letters with a tilde denote the coupling variables associated with the agent undergoing optimization, whereas letters without a tilde represent the corresponding values previously determined by other agents. The iterative refinement of exchange prices for electricity and gas flexibility services, incorporating deviations in coupling variables, is addressed in lines 12 and 13. To assess the algorithm's progress, primal residuals, quantifying inconsistencies in coupling variables, are computed in lines 14 and 15, while dual residuals, capturing variations in price updates, are derived in lines 16 and 17. An adaptive mechanism (lines 19–25) modulates penalty coefficients based on the relative magnitudes of these residuals. If the primal residual significantly exceeds the dual residual, the penalty coefficient is logarithmically increased, while the opposite case results in a logarithmic reduction. This adaptive tuning allows the framework to dynamically respond to system variations, achieving faster and more stable convergence compared to traditional ADMM methods with fixed parameters. Finally, the stopping criteria, defined in line 26, ensure termination when the cumulative sum of primal and dual residuals falls

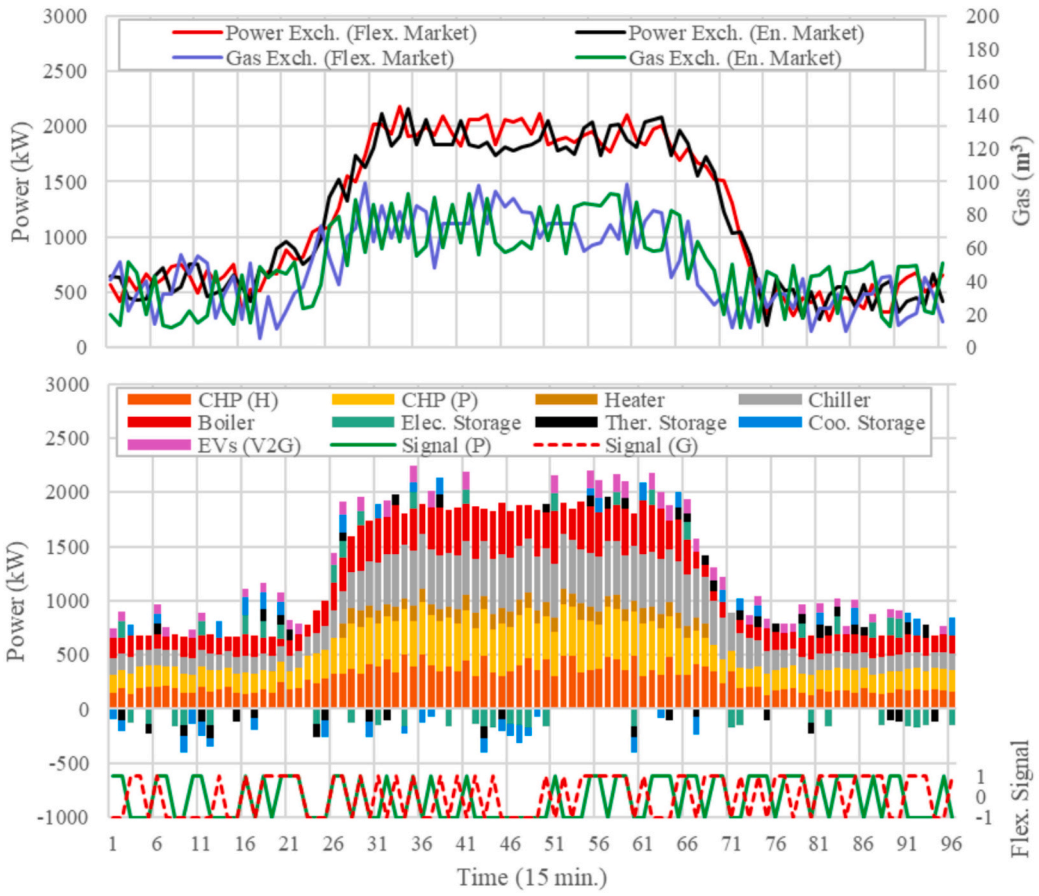

Fig. 8. Program obtained for the residential hub.

below a predefined threshold of 0.001, guaranteeing global optimality.

Algorithm 1. Pseudocode for executing the proposed ADMM.

1. **Set** initial values for the optimal operation point of energy hubs
2. **Set** initial values for penalty coefficients
3. **Set** initial values for service prices;
4. **Introduce** $P_{h,t}^{Hub}$ and $G_{h,t}^{Hub}$ based on the previous day's power ($\overline{P}_{h,t}^{Hub}$) and gas ($\overline{G}_{h,t}^{Hub}$) exchanges and the current day's services:
   $P_{h,t}^{Hub} = \overline{P}_{h,t}^{Hub} + P_{h,t}^{Hub,D} - P_{h,t}^{Hub,U}$
   $G_{h,t}^{Hub} = \overline{G}_{h,t}^{Hub} + G_{h,t}^{Hub,D} - G_{h,t}^{Hub,U}$
5. **Add** penalty term to objective function (1);
   $F^{SO,ADMM} = F^{SO} + \frac{\rho_h^P}{2}\left\|P_{h,t}^{Hub} - \widetilde{P}_{h,t}^{Hub}\right\|_2^2 + \frac{\rho_h^G}{2}\left\|G_{h,t}^{Hub} - \widetilde{G}_{h,t}^{Hub}\right\|_2^2$
6. **Add** penalty term to objective function (2);
   $F_h^{Hub,ADMM} = F_h^{Hub} + \frac{\rho_h^P}{2}\left\|P_{h,t}^{Hub} - \widetilde{P}_{h,t}^{Hub}\right\|_2^2 + \frac{\rho_h^G}{2}\left\|G_{h,t}^{Hub} - \widetilde{G}_{h,t}^{Hub}\right\|_2^2$
7. **Repeat**;
8. **Solve** the system operator optimization problem with objective (1) and constraints (a1)-(d6);
9. **For** energy hub h, **Do**:
10. **Solve** optimization problem of energy hub ***h*** with objective (2) and constraints (e1)-(g6);
11. **End**;
12. **Update** service prices for power;
    $\lambda_{h,t}^{P,Hub} = \lambda_{h,t}^{P,Hub} + \rho_h^P\left(P_{h,t}^{Hub} - \widetilde{P}_{h,t}^{Hub}\right)$
13. **Update** service prices for gas;
    $\lambda_{h,t}^{G,Hub} = \lambda_{h,t}^{G,Hub} + \rho_h^G\left(G_{h,t}^{Hub} - \widetilde{G}_{h,t}^{Hub}\right)$
14. **Calculate** primal residuals for power exchanges;
    $PR^P = \left\|P_{h,t}^{Hub} - \widetilde{P}_{h,t}^{Hub}\right\|_2$

(*continued on next column*)

(*continued*)

15. **Calculate** primal residuals for gas exchanges;
    $PR^G = \left\|G_{h,t}^{Hub} - \widetilde{G}_{h,t}^{Hub}\right\|_2$
16. **Calculate** dual residuals for power exchanges;
    $DR^P = \left\|\rho_h^P\left(P_{h,t}^{Hub} - \widetilde{P}_{h,t}^{Hub}\right)\right\|_2$
17. **Calculate** dual residuals for gas exchanges;
18. $DR^G = \left\|\rho_h^G\left(G_{h,t}^{Hub} - \widetilde{G}_{h,t}^{Hub}\right)\right\|_2$
19. **If** $PR^{P/G} \gg DR^{P/G}$, **Then**:
20. Increase the penalty coefficients using term $\gamma \log^{\alpha PR^{P/G}/DR^{P/G}}$;
21. **ElseIf** $DR^{P/G} \gg PR^{P/G}$,**Then**:
22. Decrease the penalty coefficients using term $\gamma \log^{\alpha DR^{P/G}/PR^{P/G}}$;
23. **Else**
24. Keep the previous Values for $\rho_h^{P/G}$;
25. **End**;
26. **Until** $PR^P + DR^P + PR^G + DR^G \leq 0.001$;

The proposed logarithmic coefficient update addresses the fundamental ADMM trade-off between primal and dual convergence rates [57]. Traditional approaches use either: (i) fixed coefficients maintaining $O(1/k)$ convergence but requiring manual tuning, or (ii) linear updates $\rho^{(k+1)} = \rho^{(k)}.(PR/DR)$, achieving faster convergence but risking instability when residual ratios become large [58]. The logarithmic function with adaptive exponent provides bounded, smooth adaptation that combines the advantages of both. Mathematically, when primal residuals dominate (e.g., $PR/DR = 100$, linear scaling yields $\rho^{(k+1)} = 100\rho^{(k)}$ (explosive growth causing oscillations), while the logarithmic update provides controlled adaptation through bounded growth. Under

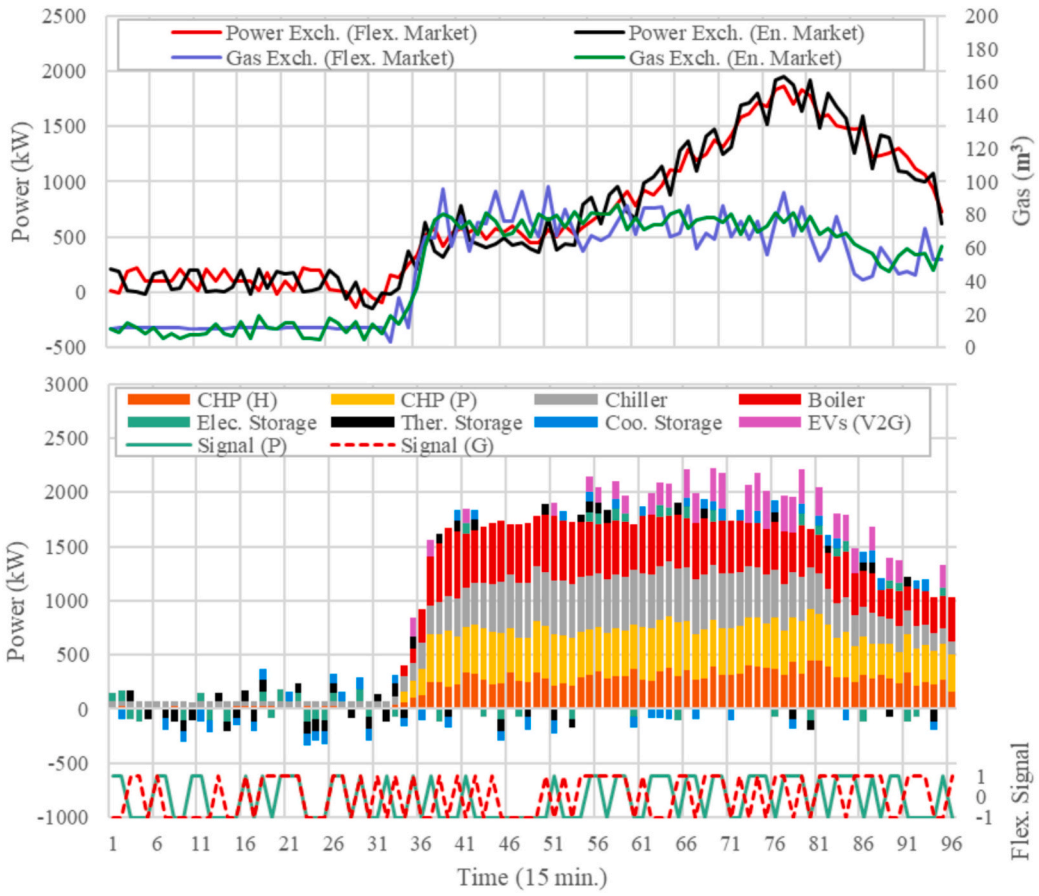

Fig. 9. Program obtained for the commercial hub.

standard ADMM convexity assumptions, this yields theoretically faster $O(1/k^2)$ convergence compared to $O(1/k)$ for fixed methods [59].

Implementation Details: In Algorithm 1, γ is the base scaling coefficient controlling the overall adaptation magnitude, and σ is the exponential weight parameter that modulates the residual ratio (PR/DR or DR/PR) before applying the logarithmic transformation. The logarithm uses the natural base (e). Initial penalty coefficients are set to $\rho_h^P(0) = \rho_h^G(0) = 1$, with bounds $\rho \in [0.01, 100]$ to prevent numerical instabilities. Updates are triggered when the residual ratio exceeds the threshold of 10 (i.e., $PR/DR > 10$ or $DR/PR > 10$).

4. Simulation results

The proposed model is implemented using the GUROBI solver within the GAMS environment and applied to the coupled power-gas system depicted in Fig. 3. This system comprises a 118-bus power distribution network and a 65-node gas distribution network, which are coupled with 18 residential, 14 commercial, and 11 industrial energy hubs. The system includes three gas-fueled dispatchable units, three wind power units, sixteen PV units, nineteen electrical storage systems, four gas storage systems, and two gas booster compressors, all managed by the system operator. Input datasets used in the simulation are available in [60]. To evaluate the effectiveness of the proposed model in optimizing the flexible capacities of electrical and gas storage systems, as well as the advanced demand-side technologies within energy hubs, five case studies have been formulated. The structure and specifications of these case studies are outlined in Table 2.

In Case 1, the system operator relies exclusively on external networks and dispatchable generation units to meet the flexibility requirements of the power and gas networks. In Case 2, system-level electrical and gas storage systems are integrated into these resources. The numerical results in Table 3 indicate that incorporating storage systems in Case 2 reduces the system operator's dependence on external networks for flexibility provision by 10.09% while lowering total daily costs for energy imbalance management by 8.36%. Figs. 4 and 5 illustrate the contribution of various resources to flexibility provision in the power and gas networks under both cases. The results confirm that activating electrical and gas storage systems reduces reliance on external electricity and gas networks while enhancing system flexibility. Additionally, storage systems provide both upward and downward flexibility, demonstrating their adaptability to operational requirements.

Fig. 4 illustrates that dispatchable units contribute solely to the upward capacity of the power network, while storage systems and the external network provide both upward and downward capacities. The system operator prioritizes reducing power imports during periods of downward capacity demand over adjusting dispatchable unit output, as this strategy minimizes losses and enhances both energy and economic efficiency.

Similarly, Fig. 5 indicates that dispatchable units do not support the gas network's upward capacity, as their operation is not required. Instead, the operator maintains high local generation levels while optimizing exchanges with the external gas network, further improving overall efficiency. Additionally, Fig. 5 confirms that dispatchable units provide downward flexibility for the gas network only when upward flexibility is needed in the power network.

In Cases 3 to 5, energy hubs participate as providers of upward and downward flexibility services in the market. Specifically, Case 3 considers the activation of energy hubs solely through IDR mechanisms,

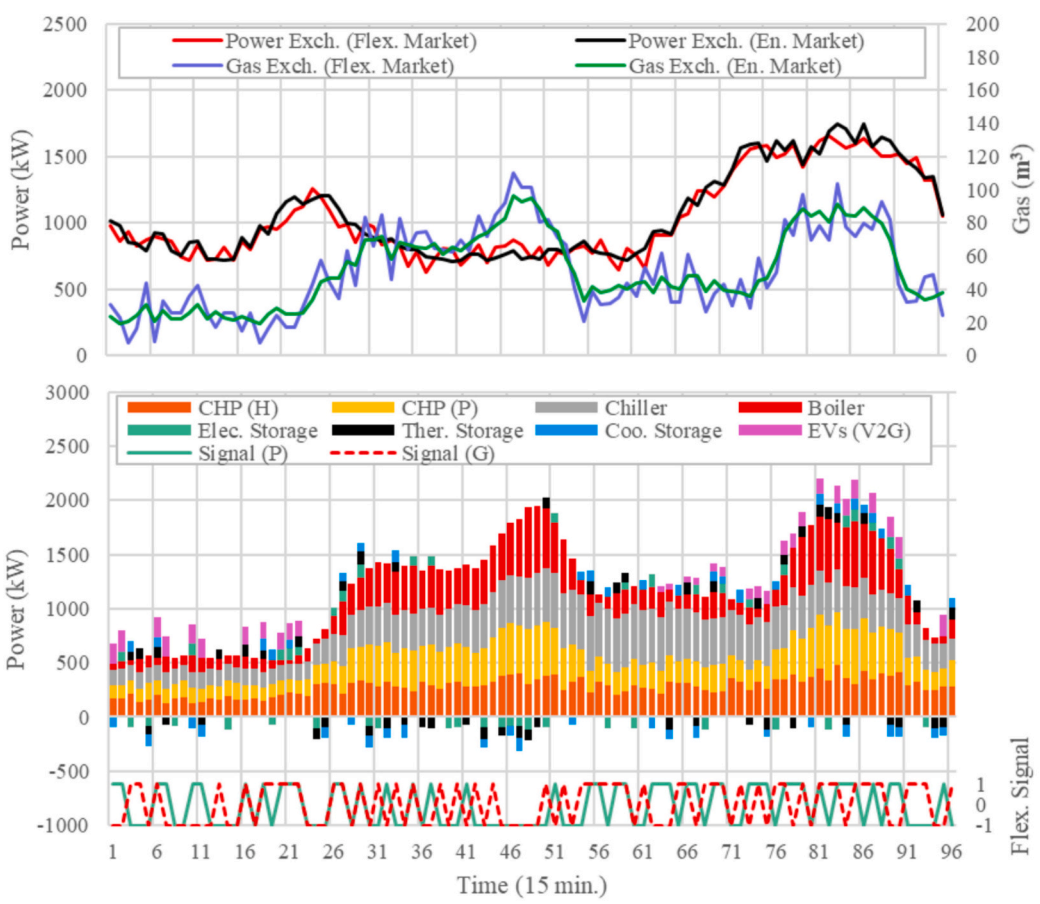

Fig. 10. Program obtained for the industrial hub.

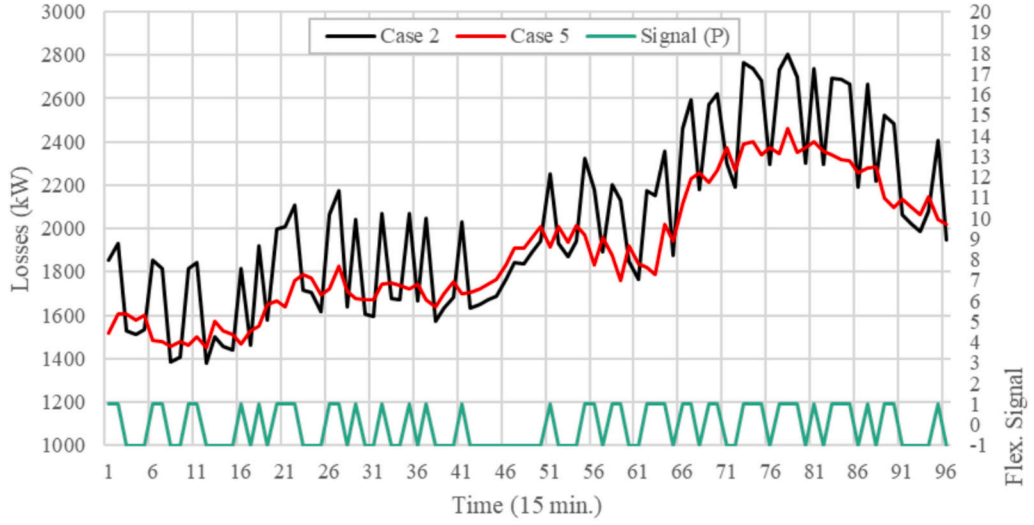

Fig. 11. Power network losses.

Case 4 incorporates both IDR and various storage systems, and Case 5 integrates all three elements: IDR mechanisms, storage systems, and V2G services. The numerical results presented in Table 3 indicate that the flexibility services offered by energy hubs via IDR mechanisms not only yielded a total profit of $5756.02 but also reduced the system operator's costs for mitigating energy imbalances by 8.6% compared to Case 2, where hubs did not provide any services. Furthermore, the activation of storage systems and V2G services in Cases 4 and 5 resulted in a revenue increase of 20.37% and 33.26%, respectively, for energy hubs relative to Case 3. The findings also demonstrate that the

Table 4
Contributions of flexibility technologies to system improvements.

Technology	*Cost Reduction*	*Loss Reduction*
IDR	8.60%	0.8%
Storage	3.87%	2.2%
V2G	8.18%	3.1%
Total	19.33%	6.13%

Table 5
Sensitivity Analysis of ADMM Penalty Coefficients.

Initial ρ	*Iterations*	*Time (s)*	*Total Cost*
0.1	286	3418.62	34,350.91
1 (Baseline)	172	2073.94	34,350.43
10	141	1862.37	34,350.38
100	159	2149.86	34,350.47

availability of more cost-effective demand-side flexibility in Cases 3 and 4 led to an 8.6% and 3.8% reduction, respectively, in the system operator's incurred costs.

Figs. 6 and 7 illustrate the suppliers of flexibility capacities in the power and gas networks for Case 5, respectively. A comparison with the results from Case 2 reveals that the full participation of energy hubs in the flexibility market, utilizing all available technologies, significantly reduces the system operator's dependence on external power and gas networks. The results indicate that energy hubs contribute to both upward and downward flexibility services required by the power and gas networks, leveraging their access to a diverse combination of generation components, storage systems, and flexible loads. This resource diversity enables hub operators to adjust their power and gas exchanges with the system by modifying internal planning strategies, thereby enhancing their adaptability to system operator requirements. The analysis of Figs. 6 and 7 highlights that, among different hub types, industrial hubs provide the highest flexibility services to the market, followed by commercial and residential hubs. The greater participation of industrial hubs stems from their higher flexibility in load adjustments, as well as their larger production capacities and more extensive storage systems. In contrast, residential hubs, characterized by smaller equipment sizes and lower flexibility in modifying load patterns, exhibit the lowest participation in the flexibility market.

Figs. 8–10 compare the power and gas exchanges of energy hubs in the day-ahead energy market with the finalized exchanges in the intraday flexibility market. These figures also illustrate the flexibility signals sent by the system operator to the hubs, along with the hubs' final schedules after the flexibility market settlement. The results show that energy hubs adjusted their power and gas exchanges with respective networks precisely in response to the flexibility signals received from the system operator, increasing purchases during downward flexibility signals and decreasing them during upward signals. To achieve this, they rescheduled internal components and implemented IDR on electrical, heating, and cooling loads. This responsiveness enabled the provision of significant upward and downward flexibility capacities to the system operator. Specifically, during periods of demand for upward flexibility services in both the power and gas networks, a portion of EVs, along with electrical, cooling, and thermal storage systems, transitioned into discharge mode, while electrical, thermal, and cooling loads were curtailed under the IDR mechanism. Conversely, during periods requiring downward flexibility services, a reverse strategy was applied.

Fig. 11 compares power network losses in Cases 2 and 5, illustrating that when hubs leverage all available advanced technologies in the flexibility market (Case 5), power losses are significantly reduced during periods of upward flexibility demand. This reduction is primarily due to hubs locally supplying a substantial portion of the required upward flexibility, thereby decreasing reliance on power imports from the external network and enhancing overall system efficiency.

To provide clearer insight into the individual contributions of each technology, the incremental benefits are analyzed in Table 4. Regarding cost reductions, IDR mechanisms (Case 3 vs. Case 2) reduce system operator costs by 8.60%, storage systems (Case 4 vs. Case 3) provide an additional 3.87% reduction, and V2G services (Case 5 vs. Case 4) contribute a further 8.18% reduction, totaling the 19.33% overall cost decrease. For power loss reductions, the total daily losses are 193,859.8 kWh in Case 2 and 181,978.1 kWh in Case 5, representing a 6.13% reduction. The contributions are quantified as follows: IDR contributes 0.8% loss reduction, as load shifting primarily redistributes demand temporally without adding local generation; storage systems provide 2.2% reduction through localized discharge from 19 system-level units during peak periods; and V2G delivers the largest reduction of 3.1%, as distributed EV discharge across 43 energy hubs during upward

Table 6
Sensitivity Analysis of Flexibility Prices.

Price change	*Hub Profit ($)*	*Total Cost ($)*
−20%	2146.83	36,198.72
−10%	2491.36	35,284.91
0% (Baseline)	2835.24	34,350.43
+10%	3182.77	33,610.84
+20%	3524.61	32,842.09

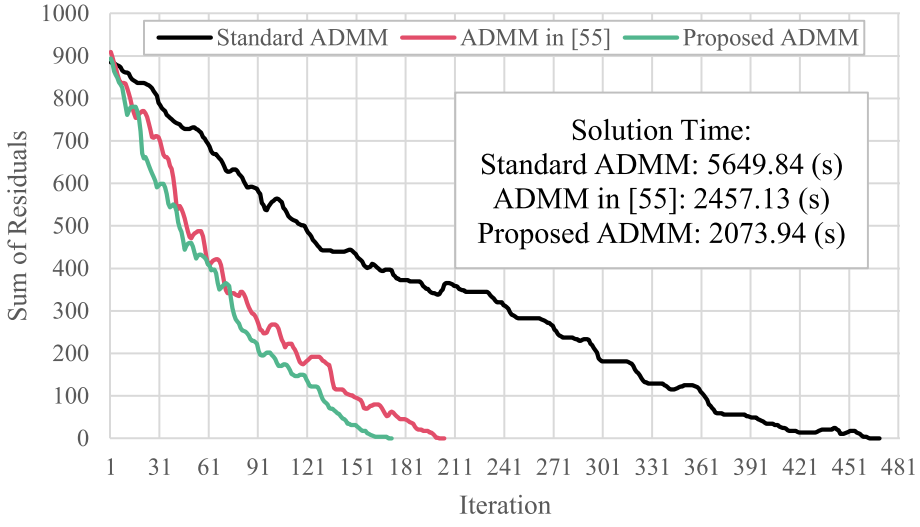

Fig. 12. Performance analysis of the proposed ADMM.

flexibility periods (periods 51–95 in Fig. 11) substantially decreases transmission distances and line currents, which is evidenced by the significant divergence between Cases 2 and 5 during high-demand hours.

Fig. 12 compares the performance of the proposed enhanced ADMM with both the standard ADMM and the adaptive version introduced in [55]. Although all three approaches reach the global optimum, the proposed version does so with substantially fewer iterations, 297 fewer than the standard ADMM and 32 fewer than the method in [55], demonstrating its improved computational efficiency. Specifically, the proposed version converges in 172 iterations, whereas the standard ADMM requires 569 iterations, and the version in [55] converges in 204 iterations. This reduction in iterations translates to computational time savings of 3575.06 s (63.27%) compared to the standard ADMM and 383.19 s (15.59%) relative to the version in [55].

To assess the robustness of the proposed adaptive ADMM algorithm and examine the economic impact of key market parameters, sensitivity analyses were conducted on the initial penalty coefficient and flexibility prices. Table 5 reports the convergence performance of Case 5 under different initial penalty values ranging from 0.1 to 100. The results indicate that the proposed algorithm consistently converges to the same global optimum, with a total cost variation of only $0.54 (0.0016%), regardless of the initial penalty value, confirming the numerical robustness of the solution.

Although the optimal objective value remains unaffected, the initial penalty coefficient has a notable impact on convergence behavior. Specifically, a small penalty value ($\rho = 0.1$) leads to slower convergence, requiring 286 iterations and 3418.62 s. In contrast, a moderate penalty value ($\rho = 10$) achieves the fastest convergence, with only 141 iterations and a total solution time of 1862.37 s. When the penalty coefficient is excessively large ($\rho = 100$), a slight degradation in computational performance is observed, with 159 iterations and a solution time of 2149.86 s, which can be attributed to increased numerical stiffness of the subproblems. Overall, convergence time varies by approximately $\pm$29% relative to the baseline case, indicating that while the adaptive ADMM mechanism guarantees optimality, an appropriate choice of the initial penalty coefficient can substantially reduce computational burden.

Table 6 presents the sensitivity of economic outcomes to variations in flexibility prices. The results reveal a clear trade-off between energy hub profitability and total system cost. As flexibility prices increase, hub profits rise proportionally: a 20% increase in flexibility prices results in a 24.3% increase in hub revenue (from $2835.24 to $3524.61), whereas a 20% price reduction leads to a corresponding 24.3% decrease in hub profit (to $2146.83). In contrast, the system operator's total cost exhibits an inverse relationship with flexibility prices. Specifically, a 20% increase in flexibility prices reduces the total system cost by 4.4% (from $34,350.43 to $32,842.09), as stronger economic incentives promote greater flexibility provision by energy hubs, thereby reducing reliance on costly external networks and dispatchable generation units. Conversely, a 20% reduction in flexibility prices increases the total system cost by 5.4% (to $36,198.72) due to diminished flexibility participation.

These findings demonstrate that appropriately designed flexibility pricing mechanisms can achieve a mutually beneficial outcome by simultaneously improving energy hub profitability and reducing overall system costs. This highlights the critical role of market-based incentives in unlocking cost-effective demand-side flexibility and enhancing the economic efficiency of coupled power–gas energy systems.

5. Conclusion

This paper developed a decentralized optimization framework to coordinate energy hubs in flexibility markets within coupled power and gas networks. A bi-level structure was formulated, where the system operator managed flexibility needs at the upper level, while residential, commercial, and industrial energy hubs optimized their participation at the lower level. To enhance coordination efficiency, an adaptive ADMM was proposed, incorporating a logarithmic coefficient-based technique for dynamic error updating. This adaptation significantly improved convergence speed, reducing computational time by up to 63.27% compared to the standard ADMM and 15.59% compared to an adaptive version recently introduced by the authors in a conference paper. The proposed model was tested on a coupled 118-bus power and 65-node gas system, demonstrating its ability to unlock flexibility from IDR, energy storage, and V2G technologies. Simulation results showed that energy hubs reduced system operator costs by up to 19.33% while decreasing power losses by 6.12%. Overall, the results demonstrated that the proposed model not only fully harnesses the flexibility potential of advanced demand-side technologies within residential, commercial, and industrial energy hubs but also accelerates decentralized market coordination while ensuring global optimality.

This study has several limitations that suggest directions for future work. The uncertainty modeling uses white noise with predefined probability distributions (Gaussian for load demand, Beta for PV, and Weibull for wind) to represent intra-day fluctuations. While this approach captures typical operational variations, it relies on stylized representations that may not fully capture temporal correlations or extreme events in real markets. The test system scale and computational experiments, while comprehensive, do not address practical challenges such as communication delays, scalability to larger networks, or strategic participant behavior. Additionally, regulatory frameworks and market policies for fair pricing and cost allocation require further development. Future work should focus on: (i) data-driven uncertainty modeling and scenario-based approaches, (ii) large-scale system validation and computational scalability analysis, (iii) sensitivity analysis of benchmarking against alternative distributed optimization methods (e.g., ALADIN, distributed MPC), (iv) analysis of strategic behaviors and market power, and (v) development of regulatory mechanisms to support real-world deployment of coordinated power-gas flexibility markets.

CRediT authorship contribution statement

Leila Bagherzadeh: Writing – original draft, Visualization, Software, Methodology, Investigation, Data curation, Conceptualization. **Innocent Kamwa:** Writing – review & editing, Validation, Supervision, Project administration, Funding acquisition. **Atieh Delavari:** Writing – review & editing, Supervision, Project administration, Funding acquisition. **Seyed Amir Mansouri:** Writing – review & editing, Supervision, Software, Methodology.

Declaration of competing interest

The authors declare that they have no known competing financial interests or personal relationships that could have appeared to influence the work reported in this paper.

Acknowledgments

This work was supported by the Canada National Sciences and Engineering Research Council through the Laval University, Grant ALLRP567550-21.

Data availability

Data will be made available on request.

References

[1] S. Parhoudeh, P.E. López, A.K. Fard, Multi-objective stochastic–adaptive robust optimization for energy management of grid-connected energy hubs including

hydrogen and thermal storages, DGs and EVs, considering energy and reserve regulation market model, J. Energy Storage 135 (2025) 118422.
[2] L.K. Elkhidir, I. Ahmed, M. Khalid, F.S. Al-Ismail, Techno-economic optimization of multi-output energy hubs with integrated storage systems and electrolyzers, J. Energy Storage 136 (2025) 118323.
[3] B. Zeng, Y. Luo, Potential of harnessing operational flexibility from public transport hubs to improve reliability and economic performance of urban multi-energy systems: A holistic assessment framework, Appl. Energy 322 (2022) 119488, https://doi.org/10.1016/j.apenergy.2022.119488.
[4] B. Heydaryan, M. Al Khatib, N. Bajcinca, Optimal control strategy for bidirectional EV charging hubs contributing to energy market, J. Energy Storage 119 (2025) 116282, https://doi.org/10.1016/j.est.2025.116282.
[5] M. Bao, H. Hui, Y. Ding, X. Sun, C. Zheng, X. Gao, An efficient framework for exploiting operational flexibility of load energy hubs in risk management of integrated electricity-gas systems, Appl. Energy 338 (2023) 120765, https://doi.org/10.1016/j.apenergy.2023.120765.
[6] A. Zare, M. Shafie-khah, P. Siano, G.C. Lazaroiu, A systematic review of virtual power plant configurations and their interaction with electricity, carbon, and flexibility markets, Renew. Sust. Energ. Rev. 226 (2026) 116448, https://doi.org/10.1016/j.rser.2025.116448.
[7] R. Habibifar, A.S.A. Awad, M.A. Azzouz, Planning energy hubs with hydrogen and battery storage for flexible ramping market participation, J. Energy Storage 140 (2025) 119012.
[8] L. Bagherzadeh, I. Kamwa, Y.Z. Alharthi, Hybrid strategy of flexibility regulation and economic energy management in the power system including renewable energy hubs based on coordination of transmission and distribution system operators, Energy Rep. 12 (2024) 1025–1043, https://doi.org/10.1016/j.egyr.2024.06.061.
[9] Z. Yadollahi, R. Gharibi, R. Dashti, A. Torabi Jahromi, Optimal energy management of energy hub: A reinforcement learning approach, Sustain. Cities Soc. 102 (2024) 105179, https://doi.org/10.1016/j.scs.2024.105179.
[10] K. Shafiei, A. Seifi, M.T. Hagh, A novel multi-objective optimization approach for resilience enhancement considering integrated energy systems with renewable energy, energy storage, energy sharing, and demand-side management, J. Energy Storage 115 (2025) 115966, https://doi.org/10.1016/j.est.2025.115966.
[11] X. Huo, Z. Xun, Secure decentralized energy exchange in networked microgrids via blockchain and multi-agent optimization, Int. J. Electr. Power Energy Syst. 172 (2025) 111334, https://doi.org/10.1016/j.ijepes.2025.111334.
[12] C. Mu, T. Ding, M. Qu, Q. Zhou, F. Li, M. Shahidehpour, Decentralized optimization operation for the multiple integrated energy systems with energy cascade utilization, Appl. Energy 280 (2020) 115989, https://doi.org/10.1016/j.apenergy.2020.115989.
[13] W. Alharbi, K. Bhattacharya, Incentive Design for Flexibility Provisions from Residential Energy Hubs in smart grid, IEEE Trans. Smart Grid 12 (2021) 2113–2124, https://doi.org/10.1109/TSG.2021.3049291.
[14] S. Feng, W. Wei, Y. Chen, Day-ahead scheduling and online dispatch of energy hubs: A flexibility envelope approach, IEEE Trans. Smart Grid (2023) 1, https://doi.org/10.1109/TSG.2023.3337629.
[15] H. Yao, Y. Xiang, S. Hu, G. Wu, J. Liu, Optimal prosumers' peer-to-peer energy trading and scheduling in distribution networks, IEEE Trans. Ind. Appl. 58 (2022) 1466–1477, https://doi.org/10.1109/TIA.2021.3133207.
[16] M. Grzanić, J.M. Morales, S. Pineda, T. Capuder, Electricity cost-sharing in energy communities under dynamic pricing and uncertainty, IEEE Access 9 (2021) 30225–30241, https://doi.org/10.1109/ACCESS.2021.3059476.
[17] Y. Tao, J. Qiu, S. Lai, J. Zhao, Integrated electricity and hydrogen energy sharing in coupled energy systems, IEEE Trans. Smart Grid 12 (2021) 1149–1162, https://doi.org/10.1109/TSG.2020.3023716.
[18] T. Zhang, Z. Hu, Optimal scheduling strategy of virtual power plant with power-to-gas in Dual Energy Markets, IEEE Trans. Ind. Appl. 58 (2022) 2921–2929, https://doi.org/10.1109/TIA.2021.3112641.
[19] K. Ma, Y. Yu, B. Yang, J. Yang, Demand-side energy management considering Price oscillations for residential building heating and ventilation systems, IEEE Trans. Ind. Informatics 15 (2019) 4742–4752, https://doi.org/10.1109/TII.2019.2901306.
[20] H. Yang, R. Liang, Y. Zheng, S. Peng, A. Rae, E. Ackom, A. Johnston, Receding horizon optimization of power demand response for production-oriented users with real-time operating status-awareness, IEEE Trans. Consum. Electron. (2025) 1, https://doi.org/10.1109/TCE.2025.3608740.
[21] Q. Meng, Y. He, S. Hussain, J. Lu, J.M. Guerrero, Day-ahead economic dispatch of wind-integrated microgrids using coordinated energy storage and hybrid demand response strategies, Sci. Rep. 15 (2025) 26579, https://doi.org/10.1038/s41598-025-11561-2.
[22] K. Ma, J. Yang, P. Liu, Relaying-assisted Communications for Demand Response in smart grid: Cost modeling, game strategies, and algorithms, IEEE J Sel Areas Commun 38 (2020) 48–60, https://doi.org/10.1109/JSAC.2019.2951972.
[23] Y. Yao, J. Zhang, P. Miao, L. Zhang, G. Chen, F. Shu, K.-K. Wong, Hybrid RIS-enhanced ISAC secure systems: Joint optimization in the presence of an extended target, IEEE Trans. Commun. 73 (2025) 15688–15704, https://doi.org/10.1109/TCOMM.2025.3610218.
[24] H. Liu, S. Zhou, W. Gu, W. Zhuang, A. Zhou, L. Peng, M. Liu, Fast dynamic identification algorithm for key nodes in distribution networks with large-scale DG and EV integration, Appl. Energy 388 (2025) 125608, https://doi.org/10.1016/j.apenergy.2025.125608.
[25] D. Yang, X. Yuan, H. Gao, J. Ma, Z. Chen, FFRLS-based data-driven voltage security assessment for active distribution networks, IEEE Trans. Smart Grid 16 (2025) 5685–5688, https://doi.org/10.1109/TSG.2025.3596779.
[26] Q. Meng, S. Hussain, Y. He, J. Lu, J.M. Guerrero, Multi-timescale stochastic optimization for enhanced dispatching and operational efficiency of electric vehicle photovoltaic charging stations, Int. J. Electr. Power Energy Syst. 172 (2025) 111096, https://doi.org/10.1016/j.ijepes.2025.111096.
[27] J. Feng, Y. Yao, Z. Liu, Developing an optimal building strategy for electric vehicle charging stations: Automaker role, Environ. Dev. Sustain. 27 (2025) 12091–12151, https://doi.org/10.1007/s10668-024-05326-6.
[28] Y. Zhou, Z. Han, Q. Zhai, L. Wu, X. Cao, X. Guan, A data-and-model-driven acceleration approach for large-scale network-constrained unit commitment problem with uncertainty, IEEE Trans. Sustain. Energy 16 (2025) 2299–2311, https://doi.org/10.1109/TSTE.2025.3551314.
[29] J. Zheng, L. Zhai, M. Tao, W. Tang, Z. Li, Low-carbon economic dispatch in integrated energy systems: A set-based interval optimization with decision support under uncertainties, Prot. Control Mod. Power Syst. 11 (2026) 68–87, https://doi.org/10.23919/PCMP.2025.000183.
[30] N. Zhou, L. Luo, G. Sheng, X. Jiang, Scheduling the imperfect maintenance and replacement of power substation equipment: A risk-based optimization model, IEEE Trans. Power Deliv. 40 (2025) 2154–2166, https://doi.org/10.1109/TPWRD.2025.3572076.
[31] Abinash Singh, Balwinder Singh Surjan, Renewable energy based stability solution for grid-connected distribution system, Asian J. Water Environ. Pollut. 21 (2024) 59–67, https://doi.org/10.3233/AJW240073.
[32] Y. Xia, K. Wang, Y. Huang, T. Lin, L. Shi, F. Wu, Bounded rational decision-making modeling and analysis in local energy markets: A state-of-the-art review, Renew. Sust. Energ. Rev. 226 (2026) 116310, https://doi.org/10.1016/j.rser.2025.116310.
[33] F. Hu, H. Yang, S. Wei, H. Zhou, Y. Chen, H. Hu, Urban green technology transfer networks and green finance development: Evidence from the Yangtze River Delta, China, Pacific-Basin Financ. J. 96 (2026) 103055, https://doi.org/10.1016/j.pacfin.2026.103055.
[34] J. Zhao, W. Li, B. Zhu, P. Zhang, R. Tang, A tachograph-based approach to restoring accident scenarios from the vehicle perspective for autonomous vehicle testing, IEEE Trans. Intell. Transp. Syst. 26 (2025) 13909–13926, https://doi.org/10.1109/TITS.2025.3569850.
[35] J. Wang, H. Wang, J. Song, X. Chen, J. Guo, K. Li, X. Li, B. Huang, Knowledge-guided self-learning control strategy for mixed vehicle platoons with delays, Nat. Commun. 16 (2025) 7705, https://doi.org/10.1038/s41467-025-62597-x.
[36] T. Ji, S. Wang, J. Wang, J. Zhang, Beyond technology: Role of technology-organization-environment-human factors in autonomous driving adoption for new energy vehicles, J. Retail. Consum. Serv. 88 (2026) 104552, https://doi.org/10.1016/j.jretconser.2025.104552.
[37] Z. Qi, Y. Wang, Z. Liu, Z. Chao, Z. Dong, H. Wang, Real-time vehicle-induced response identification via crowdsourced labeling for high-frequency unlabeled sensor data, Eng. Appl. Artif. Intell. 167 (2026) 113789, https://doi.org/10.1016/j.engappai.2026.113789.
[38] A.M. Saatloo, M.A. Mirzaei, B. Mohammadi-Ivatloo, A robust decentralized peer-to-peer energy trading in community of flexible microgrids, IEEE Syst. J. 17 (2023) 640–651, https://doi.org/10.1109/JSYST.2022.3197412.
[39] W. Hua, Y. Zhou, M. Qadrdan, J. Wu, N. Jenkins, Blockchain enabled decentralized local electricity markets with flexibility from heating sources, IEEE Trans. Smart Grid 14 (2023) 1607–1620, https://doi.org/10.1109/tsg.2022.3158732.
[40] A.J.K. Al-Hassanawy, K. Zare, S. Ghassemzadeh, M. Nzari-Heris, Robust coordination of electricity and gas networks integrated with energy hubs, rooftop solar homes, and responsive loads, IEEE Access 12 (2024) 76038–76052, https://doi.org/10.1109/ACCESS.2024.3402612.
[41] Y. Ye, D. Papadaskalopoulos, Q. Yuan, Y. Tang, G. Strbac, Multi-agent deep reinforcement learning for coordinated energy trading and flexibility services provision in local electricity markets, IEEE Trans. Smart Grid 14 (2023) 1541–1554, https://doi.org/10.1109/tsg.2022.3149266.
[42] S. Wang, H. Hui, Y. Ding, J. Zhai, Decentralized demand response for energy hubs in integrated electricity and gas systems considering Linepack flexibility, IEEE Internet Things J. 11 (2024) 11848–11861, https://doi.org/10.1109/JIOT.2023.3331115.
[43] N. Liu, L. Tan, H. Sun, Z. Zhou, B. Guo, Bilevel heat–electricity energy sharing for integrated energy systems with energy hubs and prosumers, IEEE Trans. Ind. Informatics 18 (2022) 3754–3765, https://doi.org/10.1109/TII.2021.3112095.
[44] E. Valipour, R. Nourollahi, K. Zare, S.G. Zadeh, A P-robust peer-to-peer framework for multi-energy microgrids in fully renewable integrated power and gas networks, Electr. Power Syst. Res. 253 (2026) 112525.
[45] M. Mirzaei, M. Eslami, M.J. Shahbazzadeh, A. Khajehzadeh, Enhancing flexibility in a residential energy hub through integrating electric vehicle and energy saving programs, Sci. Rep. 15 (2025) 12660.
[46] X. Nie, S.A. Mansouri, A. Rezaee Jordehi, M. Tostado-Véliz, A two-stage optimal mechanism for managing energy and ancillary services markets in renewable-based transmission and distribution networks by participating electric vehicle and demand response aggregators, Int. J. Electr. Power Energy Syst. 158 (2024) 109917, https://doi.org/10.1016/j.ijepes.2024.109917.
[47] T.H.B. Huy, H. Truong Dinh, D. Ngoc Vo, D. Kim, Real-time energy scheduling for home energy management systems with an energy storage system and electric vehicle based on a supervised-learning-based strategy, Energy Convers. Manag. 292 (2023) 117340, https://doi.org/10.1016/j.enconman.2023.117340.
[48] S. Habib, S. El-Ferik, M.M. Gulzar, S.T. Chauhdary, H. Ahmad, E.M. Ahmed, Optimizing integrated energy systems with a robust MISOCP model and C&CG algorithm for enhanced grid efficiency and profitability, Energy 318 (2025) 134795.

[49] J.A. Aguado, Á. Paredes, Coordinated and decentralized trading of flexibility products in inter-DSO local electricity markets via ADMM, Appl. Energy 337 (2023) 120893, https://doi.org/10.1016/j.apenergy.2023.120893.
[50] C. Gu, J. Wang, L. Wu, Distributed energy resource and energy storage investment for enhancing flexibility under a TSO-DSO coordination framework, IEEE Trans. Autom. Sci. Eng. (2023) 1–13, https://doi.org/10.1109/tase.2023.3272532.
[51] Á. Paredes, J.A. Aguado, P. Rodrí-guez, Uncertainty-aware trading of congestion and imbalance mitigation services for multi-DSO local flexibility markets, IEEE Trans. Sustain. Energy (2023) 1–13, https://doi.org/10.1109/tste.2023.3257405.
[52] S.A. Mansouri, E. Nematbakhsh, A. Ramos, M. Tostado-Véliz, J.A. Aguado, J. Aghaei, A robust ADMM-enabled optimization framework for decentralized coordination of microgrids, IEEE Trans. Ind. Inform. (2024) 1–10, https://doi.org/10.1109/TII.2024.3478274.
[53] K. Zhang, S. Troitzsch, S. Hanif, T. Hamacher, Coordinated market Design for Peer-to-Peer Energy Trade and Ancillary Services in distribution grids, IEEE Trans. Smart Grid 11 (2020) 2929–2941, https://doi.org/10.1109/TSG.2020.2966216.
[54] L. Marques, A. Sanjab, Y. Mou, H.L. Cadre, K. Kessels, Grid impact aware TSO-DSO market models for flexibility procurement: Coordination, pricing efficiency, and information sharing, IEEE Trans. Power Syst. (2022) 1–14, https://doi.org/10.1109/TPWRS.2022.3185460.
[55] L. Bagherzadeh, S.A. Mansouri, I. Kamwa, A.R. Jordehi, A Decentralized Business Model for Integrating Energy Hubs Into Flexibility Markets Within Renewable-Based Smart Grids, Int. Conf. Smart energy Syst. Technol. 2024 (2024) 1–6, https://doi.org/10.1109/SEST61601.2024.10694534.
[56] E. Raheli, Y. Werner, J. Kazempour, Flexibility of integrated power and gas systems: Gas flow modeling and solution choices matter, IEEE Trans. Power Syst. 40 (2024) 2130–2142.
[57] J. Yuan, Y. Wang, H. Ma, W. Liu, Federated logistic regression with enhanced privacy: A dynamic Gaussian perturbation approach via ADMM from an information-theoretic perspective, Entropy 27 (2025) 1148.
[58] M. Hasanzadeh, A. Kargarian, ADMM enhancement techniques for distributed optimal power flow, IEEE Trans. Power Syst. 40 (2025) 1–14.
[59] H.-N. Nguyen, Optimal parameter selection for ADMM: Quadratically constrained quadratic program, IEEE Trans. Autom. Control 70 (2025) 6751–6766.
[60] L. Bagherzadeh, Input Datasets (n.d.), https://www.leepci.com/resources/datasets#h.9th9hfpy5yjp, 2026.